

# Investigation of the internal heat transfer in GREC

– TMPE09 - Project Report

Johan Hagströmer, johha337  
Mattias Reijm, matre315  
Oscar Torsteinstrud, oscto185  
Vendela Stenholm, venst050

# Abstract

The GREC is a new engine under development of nilsinside AB. As a conventional Sterling engine, it uses sources with different temperatures to firstly generate a pressure difference that in turn can generate work. The advantage of the GREC is that it has a large heating area per volume and easily can be scaled up. These attributes offer the possibility to increase the work output.

Within this project, the characteristics of the heat transfer related to the GREC are investigated to understand how the pressure difference and the work depends on the used settings and design. It will also be studied if and how an increase of turbulent flow can enhance the performance of the GREC. This work will be done by creating a model that can simulate the fluid flows and the heat transfer in COMSOL.

The performance of the GREC depend on a number of parameters. A high pressure difference in the GREC does not directly implies a high work output. If high work output is desired, reaching a high heat transfer coefficient (HTC) is important. This can be done by increasing the rotation speed, having a longer rotor radius, using HTC optimizers and applying a 1/8 RS design. These configurations conduct in higher generated work. To achieve a higher work output, more heat and cooling must also be available.

The design proposal for the future is to build an engine that match the specific objective and preconditions for a special case. A large rotor radius is desirable if large amounts of work is desired and the delivering of heat and cooling is no problem. Future work is important to evaluate the performance of the GREC in regards to other parameters not brought up within this project e.g., the number of layers used.

# Preface / Préface

We want to seize this opportunity to express our gratitude towards nilsinside AB and Nils Karlberg for letting us work together with the development of the exiting GREC technology this autumn. It has expanded our knowledge not only in regards to the technology behind the GREC but also when it comes to entrepreneurship and early stage development of a new product. Nils has inspired us with his commitment and interest in our work. We all hope to be able to have a chance to sit down for a Swedish "fika", involving an espresso and not the traditional filter coffee that we have in Sweden, when he arrives home after spending the winter months in France.

Moreover, we would also like to thank Sophia Karlberg, the CEO of nilsinside AB, and Rickard Solsjö for helping us with our work to reach the result that we today present to you. It is also in its place to send our gratitude to Markus Eriksson, Oscar Magnusson, Lukas Haglund, John Malmdal and Gustav Edholm for helping us in our work through their own previous work. This work has been one of the building blocks for our own report and we are thankful for them letting us use their data, figures and knowledge.

Further we would like to thank Johan Renner, our supervisor, for showing great interest in our work and acting as a ballpark whenever we have needed. The discussion we have had have been more than helpful and have brought up a lot of new perspectives and ideas. Lastly, the second half of our group from Linköpings university, working with a different project connected to the GREC, should also be mentioned here. This group consisting of Maja Abrahamsson Bolstad, Emma Anderrson, Emma Gustafsson, Matilda Eriksson and Wilma Fager have helped us deliver this result and has also contributed to a good and interesting discussion around the GREC technology.

*Nous voulons saisir cette occasion pour exprimer notre gratitude envers nilsinside AB et Nils Karlberg pour nous avoir permis de travailler ensemble sur le développement de la technologie GREC cet automne. Cela a élargi nos connaissances non seulement en ce qui concerne la technologie derrière le GREC mais aussi en ce qui concerne l'esprit d'entreprise et le développement précoce d'un nouveau produit. Nils nous a inspiré par son engagement et son intérêt pour notre travail. Nous espérons tous avoir la chance de pouvoir nous asseoir pour un "fika" suédois, impliquant un espresso et non le traditionnel café filtre que nous avons en Suède, lorsqu'il rentrera chez lui après avoir passé les mois d'hiver en France.*

*Par ailleurs, nous tenons également à remercier Sophia Karlberg, le PDG de nilsinside AB, et Rickard Sjöberg pour nous avoir aidé dans notre travail afin d'arriver au résultat que nous vous présentons aujourd'hui. Il est également de mise d'adresser notre gratitude à Markus Eriksson, Oscar Magnusson, Lukas Haglund, John Malmdal et Gustav Edholm pour nous avoir aidé dans notre travail grâce à leurs propres travaux antérieurs. Ces travaux ont été l'un des fondements de notre propre rapport et nous leur sommes reconnaissants de nous avoir permis d'utiliser leurs données, leurs chiffres et leurs connaissances.*

*Nous tenons également à remercier Johan Renner, notre superviseur, pour l'intérêt qu'il a porté à notre travail et pour nous avoir servi de point de repère à chaque fois que nous en avons eu besoin. Les discussions que nous avons eues ont été plus qu'utiles et ont apporté beaucoup de nouvelles perspectives et idées. Enfin, la seconde moitié de notre groupe de l'université de Linköpings, qui travaille sur un autre projet lié au GREC, doit également être mentionnée ici. Ce groupe composé de Maja Abrahamsson Bolstad, Emma Anderrson, Emma Gustafsson, Matilda Eriksson et Wilma Fager nous a aidé à obtenir ce résultat et a également contribué à une discussion intéressante autour de la technologie GREC.*

# Nomenclature

## Abbreviations & Acronyms

CFD	Computational Fluid Dynamics
CHT	Conjugate Heat Transfer
EVR	Eddy Viscosity Ratio ( $\mu_t/\mu$ )
GCI	Grid convergence index
GREC	Green Revolution Energy Converter
HTC	Heat transfer coefficient
RS	Revolving shutter
WGV	Work Generating Volume

## Symbols

$\dot{Q}$	Rate of heat flow	[W]
$\dot{q}$	Heat flux	[W/m <sup>2</sup> ]
$\dot{W}$	Work	[W]
$\mu$	Dynamic viscosity	[kg/m · s]
$\mu_t$	Eddy Viscosity	[kg/m · s]
$\nu$	Kinematic viscosity	[m <sup>2</sup> /s]
$\Omega$	Angular frequency	[rad/s]
$\rho$	Density	[kg/m <sup>3</sup> ]
A	Area	[m <sup>2</sup> ]
$C_p$	Specific heat capacity at constant pressure	[J/kg · K]
h	Heat transfer coefficient	[W]
K	Design factor	[-]
L	Number of layers	[-]
m	Mass	[kg]
N	Revolution speed	[RPM]
p	Pressure	[Pa]
R	Gas constant	[J/kg · K]
r	Radius	[m]

T	Temperature	[K]
t	WGV thickness	[m]
V	Volume	[m <sup>3</sup> ]
W	Work	[J]

# Contents

<b>1</b>	<b>Introduction</b>	<b>1</b>
1.1	GREC . . . . .	1
1.1.1	Technical overview . . . . .	1
1.1.2	Development . . . . .	2
1.2	Objective and Specific Aims . . . . .	3
1.3	Limitations . . . . .	3
<b>2</b>	<b>Theory</b>	<b>4</b>
2.1	Carnot cycle . . . . .	4
2.2	Technology of the GREC . . . . .	5
2.2.1	Available work . . . . .	7
2.3	Computational Fluid Dynamics . . . . .	8
2.3.1	Turbulence modeling . . . . .	9
2.3.2	Reynolds number for WGV . . . . .	9
2.3.3	Heat transfer coefficient . . . . .	10
2.4	GCI-Method . . . . .	11
<b>3</b>	<b>Method</b>	<b>13</b>
3.1	Domain description . . . . .	13
3.1.1	Domain simplification . . . . .	13
3.1.2	Computational domain . . . . .	14
3.1.3	Mesh . . . . .	16
3.2	Simulations . . . . .	17
3.2.1	Verification and choice of mesh . . . . .	19
3.2.2	Design of revolving shutter . . . . .	19
3.2.3	Potential of optimizing the HTC . . . . .	20

3.2.4	Transient simulation . . . . .	21
3.2.5	Validation run . . . . .	22
3.3	Post-processing . . . . .	22
3.3.1	Pressure and temperature . . . . .	22
3.3.2	Heat transfer coefficient and rate of heat flow . . . . .	23
3.3.3	Calculation of work . . . . .	24
<b>4</b>	<b>Results</b>	<b>25</b>
4.1	Results for verification and validation . . . . .	27
<b>5</b>	<b>Discussion</b>	<b>28</b>
5.1	Method and model . . . . .	28
5.1.1	Mesh . . . . .	29
5.1.2	Verification . . . . .	29
5.1.3	Validation of model . . . . .	30
5.1.4	Work output calculations . . . . .	31
5.2	Parameter study . . . . .	32
5.2.1	Rotor speed . . . . .	32
5.2.2	Rotor radius . . . . .	33
5.2.3	Thickness of WGV . . . . .	33
5.2.4	Changed design of revolving shutter . . . . .	33
5.2.5	Use of HTC optimizers . . . . .	34
5.3	Future work . . . . .	35
<b>6</b>	<b>Conclusions</b>	<b>37</b>

# 1 Introduction

The debate of climate change in the society is increasing in temperature along with the climate itself. From the melting glaciers in Antarctica, extreme weather events in Asia and worse droughts in Europe, everyone is affected by the ongoing climate crisis [1, 2, 3]. All parts of society has to change and we all have to make an effort to reduce our impact on the global warming. Because how human use of fossil fuels and thereby emissions of greenhouse gases, we contribute to global warming [4]. Solutions from all different areas in our society must be considered to reduce our impact, a task that is far from easy. The complexity of this turns out to be greater than we might imagine since no bigger improvements has happened since the Paris Agreement was signed by 196 UN countries in 2015 [5, 6]. From this the signals are clear, the change to a sustainable future can not only be driven by politicians. Luckily, there are companies and people that thrive on the challenge to show the world that a transition to a world not based on fossil fuels is possible, and that is when we will start to talk about the GREC.

## 1.1 GREC

The Green Revolution Energy Converter (GREC) is a heat engine that is being developed by nilsinside AB [7]. An overview of the engine is presented in this chapter and a more thorough description is being presented in Chapter 2. The principle of the motor is that by moving air from a warm to a cold space, with the help of an external motor, the developed pressure differences can be used to generate more work than what is used by the motor [8]. Further, it is described that the concept is simple and has a wide variety of applications, for example the GREC could be used at an industrial site with both high and low temperature differences, and thus could be a competitive solution to today's polluting combustion engines. A strength of the GREC motor is its flexibility. It has a potential to deliver work from sources at both high and low temperature difference, making the GREC applicable in multiple places, within different types of industries and components [7].

### 1.1.1 Technical overview

The main components in the GREC is the Revolving Shutter (RS), the Work Generating Volume (WGV), the insulating nil-fins and the hot and cold blocks. These components can be seen in Figure 1. The GREC is a closed system where the WGV is an empty space containing gas, at an initial stage air. The RS is used to move the slices of the WGV between the hot and cold block in a circular motion. The RS is driven by an external motor that allows the user to adjust the speed.

If studied from the side, the GREC can be divided into two different layers. Firstly, the *generation layer* consists of the RS and the WGV. The generation layer is were the movement is happening and temperature and pressure changes. Adjacent to this, there is also the *conduction layer* that consists of the hot and cold conducting fins along with the insulating nil-fins. The components within this layer never moves and are assumed to have constant temperatures. Thus, the objective

of the conduction layer is to add and extract heat to the generation layer. These layers are alternated and the number of layers can be changed depending on the need of power output, available temperature sources and application. Another parameter that can be changed is the thickness of each layer [8].

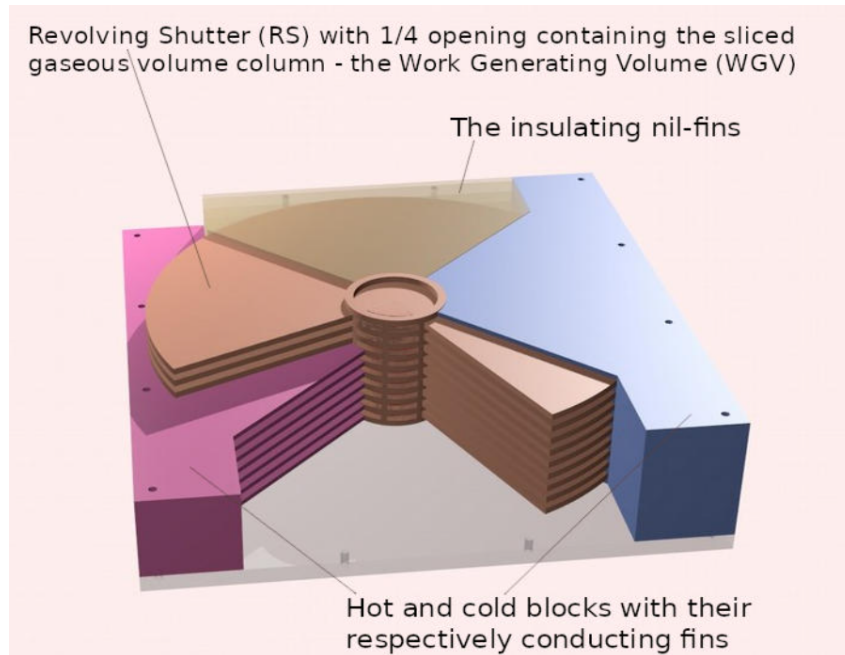


**Figure 1:** The inside of the GREC showing the Revolving Shutter (RS), the Work Generating Volume (WGV), the insulating nil-fins and the hot and cold blocks with their respectively conducting fins [9].

The thickness of each layer and especially the thickness of the WGV will affect the heat transfer within the system. The WGV is heated and cooled while it passes the conducting fins. Not only is the heat transfer dependent on the thickness of the WGV but also on its speed. The hot and the cold block respectively, will cause a fluctuating temperature difference relative to the WGV that leads to a pressure difference within the system. This pressure difference within the system, is what can be used to create work. Extraction of work could be done by using e.g. a piston that is placed somewhere suitable on the system boundary. When the internal pressure increases, as the WGV is heated up on the hot side, and exceeds the pressure in the system, the piston is pushed out. The opposite will then happen when the WGV reaches the cold side since the pressure inside the system will decrease and the piston will move back [8].

## 1.1.2 Development

So far, two lab prototypes of the GREC have been produced. The first prototype was able to generate a measurable pressure difference. However, since the second prototype is not yet fully operational, no results has been generated [10, 11]. This means that the GREC at the moment is at Technology Readiness Level 3, where research and design is actively done in order to show proof-of-concept [12]. To show the proof-of-concept, nilsinside AB had a collaboration with students at Linköping University in the spring of 2022 [13]. From their results, this project continues the development and proof-of-concept of the GREC with focus on the internal heat transfer. In parallel to this project, another group of students at Linköping University investigates the external heat transfer of the GREC and writes a project of their own. The long term goal is that these two projects eventually will form the basis of the next coming model that is planed to be built during spring 2023.

## 1.2 Objective and Specific Aims

The main objective of this project were to get a better understanding of the internal heat transfer of the GREC heat engine and also determine the subsequent pressure differences created by the machine. The earlier project that was done studied the theoretical feasibility of the machine [13]. However, their project did not go into detail about how the heat transfer from the hot and cold fins to the WGV works. Thus, the objective of this project was to gain the understanding of the characteristics for the heat transfer to and from the WGV, and also investigate the pressure differences in the machine. This by creating a model that can simulate the fluid flows and the heat transfer of the WGV, in the software COMSOL.

More specifically a number of aims for the project were decided upon.

- Study the effects on pressure differences, heat transfer coefficient (HTC) and work depending on the rotor speed, rotor radius and thickness of WGV.
- Study the effects on pressure difference, HTC and work depending on the shape of the rotor. Should there be one slit as a quarter of the disc, for the WGV, or two symmetrically placed slits that each take up an eighth of the disc area?
- Study the potential effects of implementing a HTC optimizer to increase the turbulent flow.

The end goal for the project was to gain enough knowledge about the internal heat transfer and pressure changes to make up the basis for a physical design proposal at the end of this year, or the beginning of 2023. This goal will hopefully be fulfilled with the additional knowledge provided from the findings of a second group, that were performing a project about the external heat transfer of the GREC.

## 1.3 Limitations

This project was a part of the course TMPE09 at Linköpings University which spans 12 ETCS credits giving each student a budget of 320 hours to spend on the project.

Everything that happens outside of the machine was not regarded in this project. How the solutions for the heating and cooling should look, of the heating and cooling fins respectively, was a parallel project in the same course. However, this means that during the stage of modelling and simulating, some assumptions had to be made in order to set the boundary conditions. In large, these assumptions were taken from previous works such as the one done by Eriksson et al. in 2022 [13].

# 2 Theory

In this chapter the basic theory of the working principles behind the GREC technology is further explained, as well as a short description of the Computational Fluid Dynamics solver. Moreover concepts and equations that will be used are explained. This will be done by presenting the theory and the appurtenant equations.

## 2.1 Carnot cycle

As mentioned earlier, the GREC is a form of heat engine which works on the same principle as the commercial Sterling engine [9]. Heat engines work in a cyclic pattern meaning that they always return to the same initial state at the end of each rotation. Two problems with these engines are the inevitable losses and the reversibility. However, there is a theoretical cycle that ignores the irreversibility and presents a completely reversible cycle for heat engines, namely the Carnot cycle presented by the French scientist Sadi Carnot in 1824 [14]. This cycle thus produces the most usable work that is theoretically possible, since it is an ideal cycle. The real heat engine cycle can naturally never produce as much work as the Carnot cycle but as the Carnot cycle describes the perfect conditions it has become a standard that other heat engines can be compared against [14]. In Figure 2 below a diagram of how the Carnot cycle works can be seen. The cycle is composed of four reversible processes and with a piston cylinder coupled to the volume the whole cycle can be illustrated as in the figure. The piston cylinder can also be used to extract work from the WGV. However, as mentioned in Chapter 1.3 the process of energy extraction is something that will not be covered in this work.

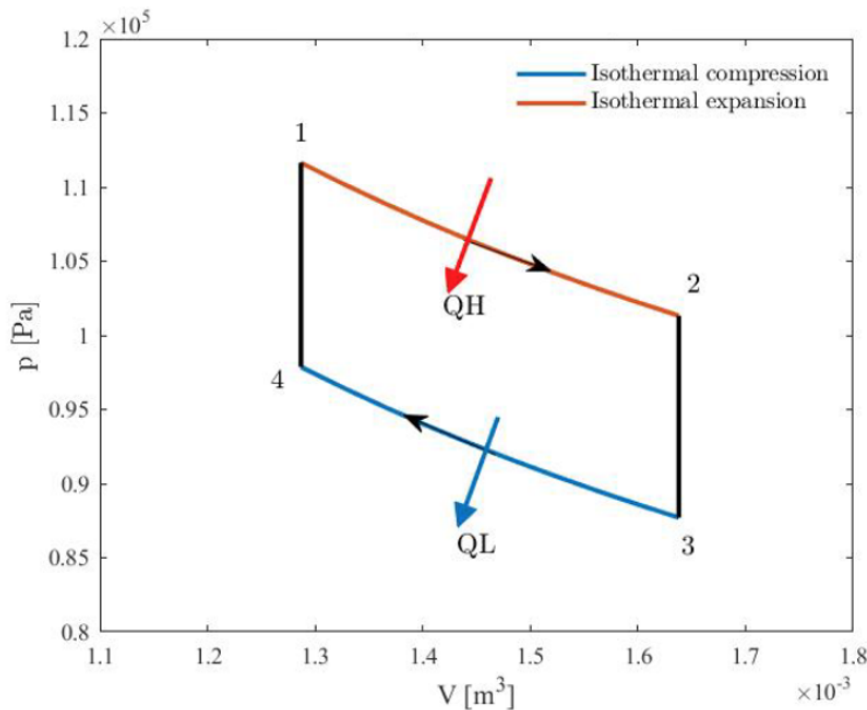
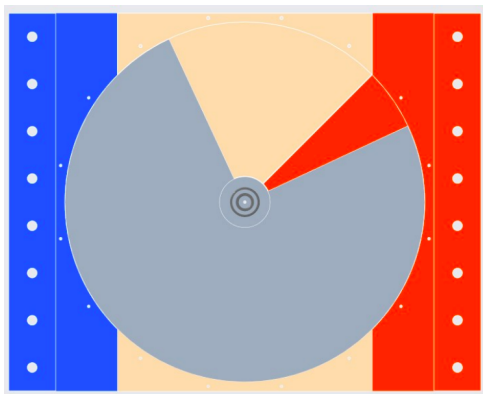


**Figure 2:** A schematic presentation that shows how the pressure and volume could change in the Carnot cycle, the values are not necessarily relevant for the current problem. The figure is obtained from Eriksson et al. [13].

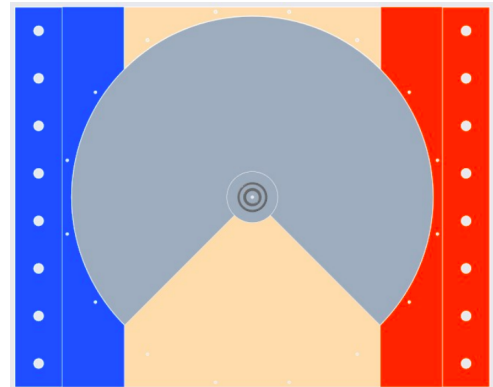
## 2.2 Technology of the GREC

To deepen the understanding of the how the GREC engine works, a more detailed description and explanation will in this chapter be presented as a complement to the technical overview in Subsection 1.1.1. In Figure 3, a schematic presentation of the RS can be seen with a clockwise rotation. The figure is divided into four subfigures representing the difference conditions that the WGV can experience. These subfigures can also be compared to the Carnot cycle in Figure 2 shown in the last chapter.

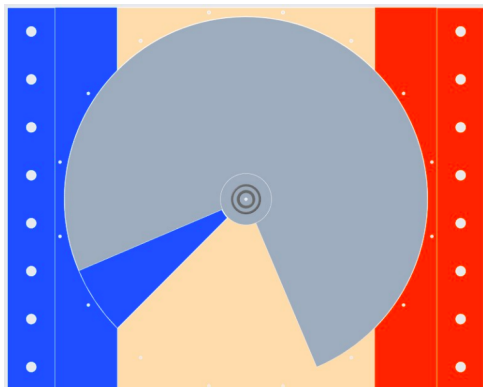
Firstly, Figure 3a shows how the WGV is in contact with the hot sink. Heat is thus transferred through convection from the heat sink to the WGV, since WGV holds a lower temperature than the heat sink, which in turn increases the temperature and pressure of the WGV. While the RS is rotating, pushing the WGV forward, the share of the WGV that is in contact with the heat sink first increases and then decreases again due to the rotational movement. The heat addition to the WGV can be thermodynamically represented by the pressure increase between point 4 and 1 in Figure 2. The pressure rise that the GREC experiences within the closed system, can at this point be used to for example push a piston, that is placed somewhere on the system boundary, out towards the ambient surrounding, given that the ambient pressure is lower than the pressure within the GREC. This expansion of the volume of the closed system will lead to a decreased pressure, meanwhile the temperature will stay high. The expansion is represented by the volume increase between point 1 and 2 in Figure 2.



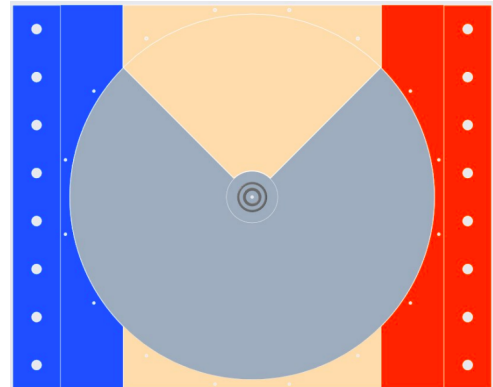
(a) The WGV is entering the hot sink.



(b) The WGV is isolated while rotating from the hot to the cold sink.



(c) The WGV is entering the cold sink.



(d) The WGV is isolated while rotating from the cold to the hot sink.

**Figure 3:** A schematic presentation, obtained from Eriksson et al. [13], showing the rotation of the RS and the WGV in a clockwise direction. The red part represents the hot sink and the blue part represents the cold sink.

After passing the hot sink, there will be a situation when the WGV is neither in contact with the hot nor the cold sink but only the insulation, this is illustrated in Figure 3b. The insulation is not contributing to the heating or cooling of the WGV. This is important to avoid that the WGV is in contact with both the hot and cold heat sink at the same time, since it would decrease the efficiency of the engine if the WGV was heated and cooled at the same time. Beyond this, the insulation is important to minimize the dead volume within the GREC. The dead volume arises due to the fact that the RS never is in contact with the surrounding walls and conducting fins. A schematic picture of the dead volume can be seen in Figure 4. By reducing the dead volume, in other words the air that is not a part of the WGV and not meant to contribute to the work generating process, the efficiency of the GREC can be increased. This comes from the fact that more dead volume implies that more of the energy, that is transferred to or from the system, has to be used to heat or cool the dead volume. Thus, that energy can not contribute to the pressure change and can in the end not be used to generate work.

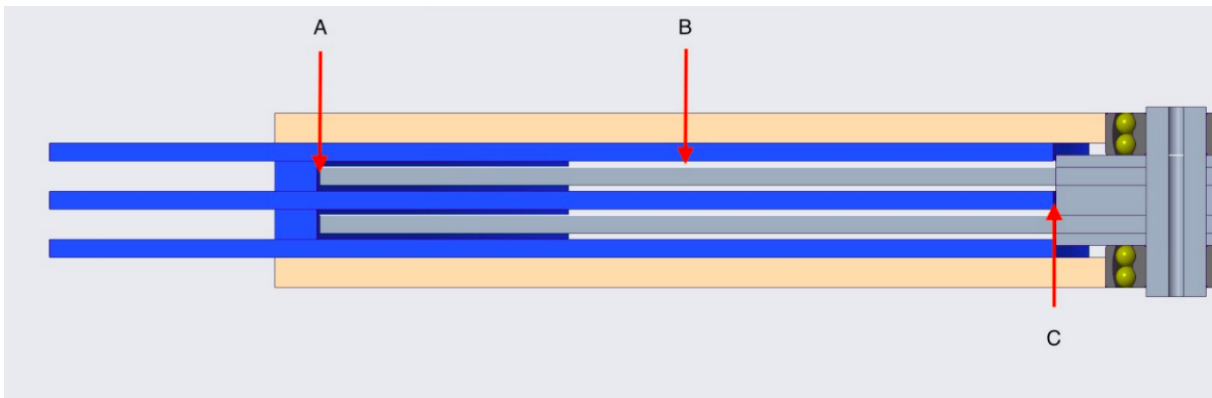


**Figure 4:** A schematic presentation, obtained from Eriksson et al. [13], of the dead volume within the GREC. (A) is the air between the RS and the surrounding wall, (B) is the air between the RS and the conducting fins and (C) is the air between the conducting fins and the shaft of the RS.

Next up, the RS rotates the WGV into contact with the cold sink, see Figure 3c. Through convection, the heat in the WGV is transferred to the colder sink thus lowering the temperature and pressure within the WGV. The heat transfer to the cold sink from the WGV can once again be thermodynamically represented in Figure 2 by the pressure drop from point 2 to point 3. Yet again, this change in pressure will move the piston. Thus, this time it will move inwards towards the system, given that the ambient pressure is higher than the pressure within the system. While the pressure is increasing, the temperature will not increase as much since the closed volume is shrunken with the moving piston. Just like over the heat sink, this piston movement can be used to generate work. This process can be represented in the Carnot cycle, Figure 2, by the compression between point 3 and 4.

Lastly, the WGV will reach the insulated section between the cold and the hot sink, see Figure 3d. This insulation has the same task as the insulation between the hot and the cold sink. When the RS repeats this cycle of moving the WGV in a rotational movement from the hot to the cold sink and then back again, the movement of the piston will also be repeated. In this way, continuous work will be generated while the piston is moving parallel to the change in pressure within the GREC.

### 2.2.1 Available work

One of the main goals of this project was to get a proposal of how much potential work is available in the GREC, as earlier mentioned in Chapter 1.2. It has been described in the earlier chapters how the temperature and pressure differences are obtained, and these differences can then produce a volume difference if the volume is connected to a movable piston cylinder. The ideal gas law was used to calculate these volume changes, see Equation (1) below [15].

$$p \cdot V = m \cdot R \cdot T \quad (1)$$

When the volume difference was known the stroke length could be calculated with Equation (2), given a constant diameter of the piston cylinder.

$$dV = A \cdot ds \leftrightarrow ds = \frac{dV}{A} \quad (2)$$

The stroke length is important for the design proposal. However, the potential work is also desirable knowledge for the project and further research on the GREC technology. Assuming that there are no losses, the available work is the work that the volume change produces i.e boundary work which is defined below in Equation (3) [15].

$$W_{12} = \int_1^2 p \cdot dV \quad (3)$$

With the assumption that the temperature is constant the boundary work equation could be rewritten as Equation (4) with the help of the ideal gas law [15].

$$W_{12} = p_1 \cdot V_1 \cdot \ln \frac{V_2}{V_1} = p_2 \cdot V_2 \cdot \ln \frac{V_2}{V_1} \quad (4)$$

Looking at Figure 2 of the Carnot cycle the boundary work for the expansion can be calculated between points 1 and 2 giving the Equation (5).

$$W_{\text{out}} = W_{12} = p_1 \cdot V_1 \cdot \ln \frac{V_2}{V_1} \quad (5)$$

Looking at the compression instead it can be seen in Figure 2 that the process is between point 3 and 4 meaning that the boundary work can be calculated as shown in Equation (6).

$$W_{\text{in}} = W_{34} = p_4 \cdot V_4 \cdot \ln \frac{V_3}{V_4} \quad (6)$$

This is the potential work that is available from one instance of change in pressure. When the machine is operating in a cyclical manner the pressure change will happen in each direction one or two times per rotation depending on the design choice, which is presented later in this report, see Figure 9. The power is thus determined as a function of the available boundary work and the rotational speed following Equation (7) below. The number 60 is included to translate RPM,

denoted as  $N$ , to rotations per second.  $K$  is a factor that depends on the design choice, one if it's the original design and two if it's the design shown in Figure 9b.

$$\dot{W}_{\text{potential}} = \frac{(W_{\text{out}} + W_{\text{in}}) \cdot N \cdot K}{60} \quad (7)$$

Equation (7) provides the final proposed value for the available power from the GREC. This value presupposes that all the available work in each pressure change can be extracted without any losses, for example friction. However, the motor to rotate the RS also uses power which means that this power must be subtracted from the potential power to get the usable power from the GREC, this can be seen in Equation (8), if  $\dot{W}_{\text{usable}}$  is negative no usable net power is produced.

$$\dot{W}_{\text{usable}} = \dot{W}_{\text{potential}} - \dot{W}_{\text{el}} \quad (8)$$

## 2.3 Computational Fluid Dynamics

The technology of Computational Fluid Dynamics, or CFD for short, gives the user the tools of solving complex fluid flows with numerical solutions on the computer. Thus, the user is not limited to simple problems where analytical solutions are possible. The technology and solving scheme are based on the so called Navier-stokes equations, which says three things [16].

- The mass is conserved.
- The momentum ( $x, y, z$ ) is conserved.
- The energy of the flow is conserved.

The conservation of mass in the flow, also called the continuity equation, can be described by Equation (9) which is presented below. All the equations that follow in this chapter are taken directly from the COMSOL solver [17].

$$\frac{\partial \rho}{\partial t} + \nabla \cdot (\rho \mathbf{u}) = 0 \quad (9)$$

Moving on to the second part and momentum equation. One thing that should be noted is the gradient which can be seen in Equation (10) below, this means that the equation can be split into three different equations, for directions  $x, y, z$ .

$$\rho \frac{\partial \mathbf{u}}{\partial t} + \rho (\mathbf{u} \cdot \nabla) \mathbf{u} = \nabla \cdot [-p \mathbf{I} + \boldsymbol{\tau}] + \mathbf{F} \quad (10)$$

The last equation that must be considered to determine the behaviour of the flow is the energy equations which can be seen below as Equation (11).

$$\rho C_p \left( \frac{\partial T}{\partial t} + (\mathbf{u} \cdot \nabla) T \right) = -(\nabla \cdot \mathbf{q}) + \boldsymbol{\tau} : \mathbf{S} - \frac{T}{\rho} \frac{\partial \rho}{\partial T} \bigg|_p \left( \frac{\partial p}{\partial t} + (\mathbf{u} \cdot \nabla) p \right) + \mathbf{Q} \quad (11)$$

Solving all these equations for every point in a domain will theoretically describe the fluid flow perfectly. However, this is not computationally feasible so the reality must be simplified in the model for the computer to solve the flow problem at a finite number of points in the studied domain. To solve these differential equations in this finite number of points there are a few different techniques that can be applied, such as FVM (Finite Volume Method) or FEM (Finite Element Method). Different solvers use different techniques, but COMSOL uses FEM. The general working method when solving CFD problems usually follows the steps below.

- Simplify the computational domain to save computational power.
- Create the physical domain that will be worked on.
- Choose the physics and boundary conditions that simulate the problem realistically.
- Create the computational mesh, the points where the Navier-stokes equations will be solved.
- Post processing.

### 2.3.1 Turbulence modeling

The Navier-Stokes equations could be used for modeling the turbulence, but since there is such a wide range of scales of eddies in the flow, the grid must be almost infinitely small, which makes this approach unfeasible [18]. An alternative approach is to take advantage of the random and chaotic behaviour of the flow, and its mean value. One can decompose the velocity into two parts, a steady mean value  $\mathbf{U}$ , and a fluctuating component  $\mathbf{u}'(t)$  [19]. This decomposition is called the Reynolds decomposition,  $\mathbf{u}(t) = \mathbf{U} + \mathbf{u}'(t)$ . When inserting this decomposition into the Navier-Stokes equations and rearrange the terms, the Reynolds-averaged Navier-Stokes (RANS) equation is obtained, see Equation (12) and (13) below [18].

$$\rho \frac{\partial \mathbf{U}}{\partial t} + \rho \mathbf{U} \cdot \nabla \mathbf{U} + \nabla (\overline{\rho \mathbf{u}' \otimes \mathbf{u}'}) = -\nabla P + \nabla \cdot \mu (\nabla \mathbf{U} + (\nabla \mathbf{U})^T) + \mathbf{F} \quad (12)$$

$$\frac{\partial \rho}{\partial t} + \nabla \cdot (\rho \mathbf{u}) = 0 \quad (13)$$

The term  $(\overline{\rho \mathbf{u}' \otimes \mathbf{u}'})$  is called the Reynolds stress tensor and is a term that needs to be modeled. This is usually modeled with classical turbulence models such as  $k - \epsilon$  or SST [19]. The computational cost is modest for reasonably accurate results, which has made this approach widely used in engineering flow applications [19].

### 2.3.2 Reynolds number for WGV

The flow inside the WGV is not well defined with simple equations. To our knowledge and research there is no standard equation for calculating the Reynolds number for this type of flow. The previous study done in the spring of 2022 calculated the Reynolds number by dividing the WGV into segments and calculating the Reynolds number for pipe flow in those segments [13]. That study calculated that seven out of 10 segments were above a Reynolds number of 2300,

i.e. turbulent flow, at a rotating speed of 500 rpm, for 1500 and 3000 rpm almost all segments where above 2300 [13].

In the book *Rotating Flow* by P. Childs (2011), Childs describes the power required to overcome the frictional drag for a hard disk drive [20]. This flow situation is similar to the one inside the GREC, except that there is a cavity (cut out) in the disc. In Equation (14) below the rotating Reynolds number is presented [21]. In Chapter 4 of *Rotating Flow* Childs concludes that the critical Reynolds number of this rotating disc is  $Re_{crit} = 2 \cdot 10^5$  [21].

$$Re_{\Phi} = \frac{\rho \Omega r^2}{\mu} = \frac{\Omega r^2}{\nu} \quad (14)$$

### 2.3.3 Heat transfer coefficient

Inside of the WGV most heat transfer is between a fluid and a solid surface, therefore most of the heat transfer is done through convection. Convection is a combination of conduction and fluid motion, and a faster fluid means a greater heat transfer [22]. There are two types of convection, natural and forced [22]. Forced implies that a fluid is forced over the surface and natural (free) convection is when fluid motion is caused by differences in density depending on the temperature [22]. This type of heat transfer is a complex area, but with a quite simple equation as its foundation. This equation is expressed by *Newton's law of Cooling*, which says that the convective heat transfer is proportional to the temperature difference, see Equation (15) below.

$$\dot{Q}_{conv} = hA_s(T_s - T_{\infty}) \quad (15)$$

Where  $h$  is the heat transfer coefficient, HTC, and  $A_s$  is the surface area.  $T_s$  is the surface temperature and  $T_{\infty}$  is the temperature of the fluid sufficiently far away from the surface. The HTC,  $h$ , is not a property of the fluid, but rather a parameter which is determined by variables such as surface geometry, fluid motion and properties of the fluid [22]. When rearranging the terms in Equation (15) the HTC can be calculated from the heat flux and the temperature difference, see Equation 16.

$$h = \frac{\dot{q}_{conv}}{(T_s - T_{\infty})} \quad (16)$$

In Equation (16) the heat flux can be extracted from the finished simulation model. To calculate the HTC value in CFD and CHT the only unknown is the temperature of the fluid. This can be estimated by a few different methods. Neale et al. presents three different methods. Firstly one can use a constant reference temperature ( $T_{ref}$ ) [23]. Secondly the temperature at the center of the domain ( $T_c$ ). Lastly the so called bulk temperature can be used ( $T_b$ ).

## 2.4 GCI-Method

The Grid Convergence Index, or in short GCI-method, is recommended to be applied in order to quantify the error that occurs by the discretisation in the domain [24]. By doing this, the error that an insufficient mesh could imply can be quantified. This verification is done to see if the mesh is good enough to be used within the CFD application. Several equations should be used to verify the mesh and the process can be divided into five steps [24]:

*Step 1:* A representative cell size ( $h$ ) for the domain is defined by using Equation (17):

$$h = \left[ \frac{1}{N} \sum_{i=1}^N (\Delta V_i) \right]^{1/3} \quad (17)$$

$\Delta V_i$  is the volume of the  $i$ th cell, and  $N$  the total number of cells in the domain. The average global cell size is appropriate if the global variable for the GCI-method is considered.

*Step 2:* Three different meshes, that are significantly different, is selected; a coarse mesh, a middle mesh and a fine mesh. Between the meshes, the refinement factor ( $r = h_{\text{coarser}}/h_{\text{finer}}$ ) between them should be greater than 1.3. The simulation is thereafter run were the key variables ( $\varphi$ ) is determined.

*Step 3:* The order  $p$ , while letting  $h_1 < h_2 < h_3$  and  $r_{21} = h_2/h_1$ ,  $r_{32} = h_3/h_2$ , is calculated with Equation (18).

$$p = \frac{1}{\ln(r_{21})} |\ln|\varepsilon_{32}/\varepsilon_{21}| + q(p)| \quad (18a)$$

$$q(p) = \ln \left( \frac{r_{21}^p - s}{r_{32}^p - s} \right) \quad (18b)$$

$$s = 1 \cdot \text{sgn}(\varepsilon_{32}/\varepsilon_{21}) \quad (18c)$$

$\varepsilon_{32}$  and  $\varepsilon_{21}$  is the difference between the solutions for each mesh. This can be seen in Equation (19a) and (19b).

$$\varepsilon_{32} = \varphi_3 - \varphi_2 \quad (19a)$$

$$\varepsilon_{21} = \varphi_2 - \varphi_1 \quad (19b)$$

*Step 4:* The extrapolated values  $\varphi_{\text{ext}}^{21}$  and  $\varphi_{\text{ext}}^{32}$  are calculated with Equation (20).

$$\varphi_{\text{ext}}^{21} = (r_{21}^p \varphi_1 - \varphi_2) / (r_{21}^p - 1) \quad (20a)$$

$$\varphi_{\text{ext}}^{32} = (r_{32}^p \varphi_3 - \varphi_2) / (r_{32}^p - 1) \quad (20b)$$

*Step 5:* The relative values  $e_a^{21}$  and  $e_a^{32}$  are calculated with Equation (21).

$$e_a^{21} = \left| \frac{\varphi_1 - \varphi_2}{\varphi_1} \right| \quad (21a)$$

$$e_a^{32} = \left| \frac{\varphi_2 - \varphi_3}{\varphi_2} \right| \quad (21b)$$

Lastly, the Grid Convergence Index  $GCI_{21}$  and  $GCI_{32}$  can be calculated with Equation (22).

$$GCI_{21} = \frac{1.25e_a^{21}}{r_{21}^p - 1} \quad (22a)$$

$$GCI_{32} = \frac{1.25e_a^{32}}{r_{32}^p - 1} \quad (22b)$$

# 3 Method

In this Chapter the methodology for the project is presented. The chapter starts with the description of the domain and the simplifications made on it to make it computationally feasible. Then it continues to describe the boundary conditions and inputs to simulate the real life physics, also the meshing strategy is covered. Thereafter, Section 3.2 covers which simulations that are carried out to obtain the results as well as a walk-through of the verification process and the parametric study.

## 3.1 Domain description

The whole domain can be defined as the complete GREC heat engine. The problem is that it is too big and complex to make relevant simulations on this domain with the available computational power and time frame. This means that the domain must be greatly simplified for the computational power to be sufficient for the relevant simulations.

### 3.1.1 Domain simplification

The first step of this project was to define how to simplify the computational model as much as possible. There are believed to be at least three main methods to model the GREC, which give three different system boundaries. In Figure 5 a schematic representation the three different system boundaries are presented.

The first one is to model one full layer, where the conducting fins, the revolving shutter and the WGV is modeled. The system boundary can be seen in Figure 5a. This approach is believed to be the most computational heavy since it includes both fluid flow and heat transfer in both solids and fluids. The size of the model would also contribute to a large number of nodes. If every one of these nodes were to be calculated, the computational time would increase further. The second approach were to only model the fluid inside the GREC as well as the revolving shutter. The system boundary can be seen in Figure 5b. This approach would be less computationally heavy but require more thoughts about the boundary conditions, especially the heat interface between the fin and the air. The third approach is to only consider the WGV as seen in Figure 5c. This approach is believed to be the least computationally heavy of the three, since it removes a big part of the domain. This comes at a cost that it becomes even more important to implement the boundary conditions correctly. Ultimately the last approach was chosen, the approach in Figure 5c. The main reason behind this choice was that it require the least amount of computational power of the three approaches. It is believed that the simplifications needed for the boundary conditions with this approach is quite well understood and will not cause to much of an error in the final results in relation to the computational time. A simpler and quicker model enhances the understanding since a larger number of simulations can be done during the time of the project. Thus, a more trial and error approach can be implemented.

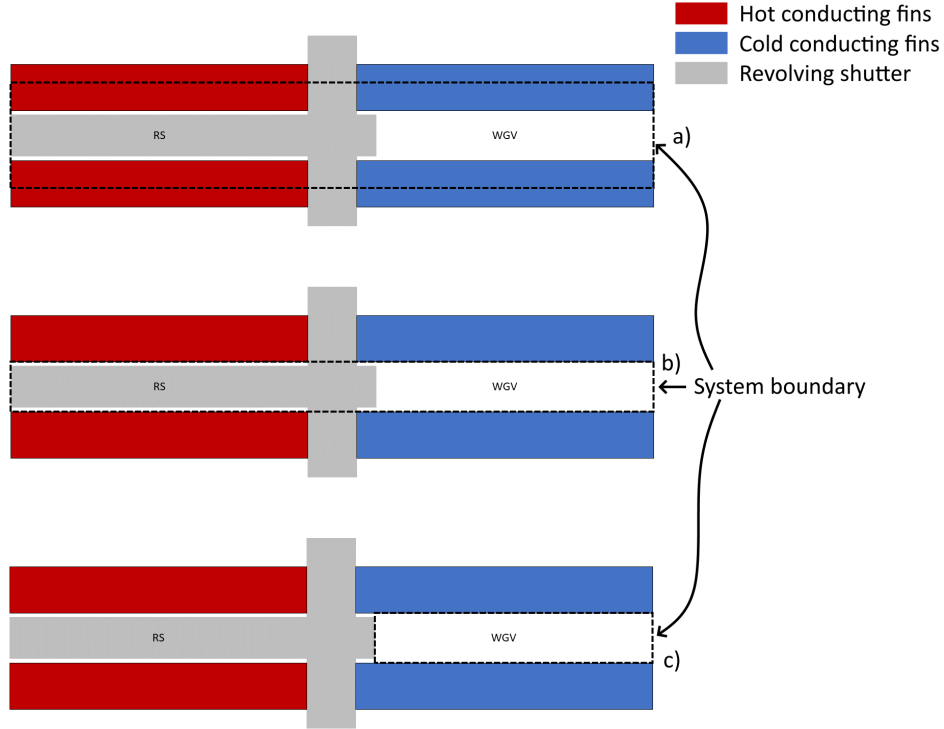


**Figure 5:** A schematic representation of three different system boundaries. a) represent a system boundary where a whole layer is taken into account. b) represents a system boundary with only the air inside the GREC and the revolving shutter. c) represents a system boundary with only the WGV taken into account.

### 3.1.2 Computational domain

To mimic the rotation of the WGV a *Rotating Domain* under the category *Moving Mesh* was inserted into the *Definitions* tab. The *Rotation type* was set to a *Specific rotational velocity* and *Rotational velocity expression* to *General revolutions per time* with a global parameter as the input. The axis of rotation were set to the Z-axis, which is the same shaft as the RS is rotating around.

The flow physics was determined by doing initial calculations on the Reynolds number from Equation (14). The flow is determined turbulent above an RPM of 500 for a diameter of 29 cm, see Table 1. Therefore a turbulence model had to be chosen. In COMSOL there are 8 different turbulence models that can be used, which all have different advantages and disadvantages [25]. Since the inside of the WGV is both internal and include heat transfer, COMSOL recommends to use a model that does not use a wall function and solves all the way down to the wall, this is true for the  $k-\omega$  model, the Low Reynolds  $k-\epsilon$  model and the SST model [25]. The SST model was ultimately chosen for its widespread use and for solving all the way down to the wall, which should compute accurate results for the heat transfer.

**Table 1:** Shows the Reynolds number for a spinning disc (Equation (14)). The flow is determined turbulent over a rotational speed of 500 RPM and a diameter of 29 cm.

Rotation speed [rpm]	Radius [m]	Reynolds number
500	0.29	$2.45 \cdot 10^5$
1500	0.29	$7.35 \cdot 10^5$
3000	0.29	$1.47 \cdot 10^6$

The compressibility was set to *Compressible flow*, which can be used when the Mach number is less than 0.3. This is fulfilled if the rotational speed is maximum 3000 rpm with a rotor radius of 29 cm, resulting in 91.1 m/s as the speed at the tip. With a speed of sound assumed to be 340.3 m/s, at sea level, the Mach number is calculated to 0.268, see Equation (23) [26].

$$\text{Ma} = \frac{v_{\text{tip}}}{v_{\text{sound}}} = 0.268 \quad (23)$$

There are two types of walls in this domain. One type has no relative movement to the air domain, i.e. the RS walls. The other type of wall is the ones that are stationary, and therefore have a relative velocity opposite of the movement of the WGV, i.e. the conducting fin walls. Therefore, two types of wall boundary conditions were implemented. On the side walls (RS walls), a *No Slip wall condition* was applied. Then a *Wall Movement* was set to *Automatic from frame* as *Transitional velocity*. On the other type of walls, the conducting fin walls, a *No Slip wall condition* was also applied. The *Wall Movement* was set to *Zero (Fixed wall)* under *Transitional velocity*. This was done to mimic the relative velocity of the wall to the WGV.

The heat transfer to and from the domain was modeled by setting a temperature boundary condition. In the real model the temperature at the walls varies with time when the air domain is the reference point. To mimic this, several *Rectangular functions* were inserted into an *Analytical function* to set the correct value at the correct time. The temperature curve was divided into four zones: one hot, one cold and two neutral representing the isolation. This is shown in Figure 6, where two full rotations are shown. It starts with a hot section, goes to neutral, to cold, to neutral and then back to hot again. The hot and cold zones were set as parameters with 100 °C and 10 °C respectively. The neutral zones were set 5 °C higher/lower than the average temperature to minimize heat transfer in these zones, i.e. make them more adiabatic/insulated.

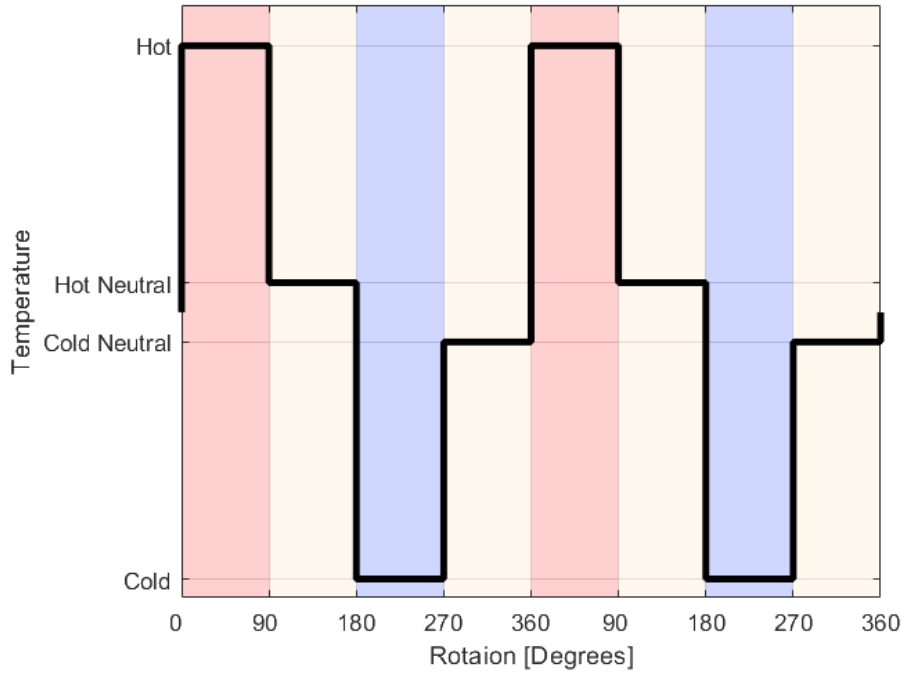


**Figure 6:** Shows the time dependent temperature boundary condition at the walls as a function of rotation for two full rotations. It is divided into four zones one hot (first step, red), one neutral (second step, yellow), one cold (third step, blue) and another neutral one (fourth step, yellow).

In Figure 7, a summary of the boundary conditions is shown. The orange walls are the walls connected to the conducting fins. The green walls are the walls connected to the RS. As seen in the figure, a symmetry plane where used for booth the heat transfer and the fluid flow. The aim of the symmetry plane is to minimize the computational cost by reducing the size of the domain and thereby also the number of elements. Thanks to the domain being symmetric it can be bisected into to identical parts, with the only difference that they are mirrored to each other over the symmetry plane. Thereby, only one of the two parts has to to be calculated by the model.

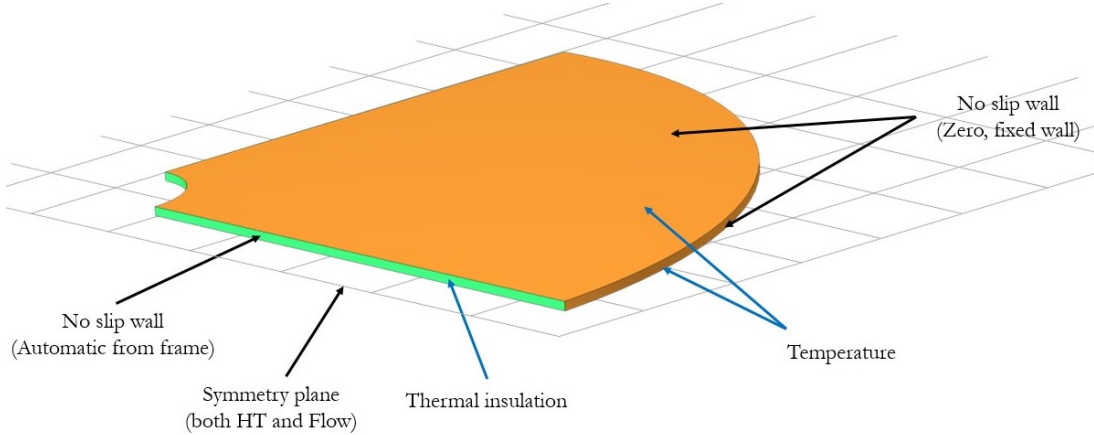


**Figure 7:** Shows the boundary conditions set on the WG. The orange walls are the walls facing the conducting fins, and the green walls are the walls facing the RS. The domain is modeled as symmetric over a symmetry plane.

### 3.1.3 Mesh

In general, the aim was to simplify the mesh as much as possible without sacrificing too much of the accuracy. Firstly a physics controlled mesh was created in COMSOL for a turbulent flow and then parameters were altered to fit the problem at hand better. The four parameters that were altered are presented below in Table 2.

**Table 2:** The size is defined as overall size and element size in COMSOL. However both are set to the same settings which can be seen below. The other three parameters has to do with the boundary layer configurations that are visualized in Figure 8a

Mesh name	Element size	Number of BL:s	First layer thickness [m]	BL stretching factor
Fine	Normal	10	0.00009	1.2
Middle	Coarse	10	0.00009	1.2
Coarse	Coarser	6	0.0002	1.2

The boundary layer configurations are applied to all walls of the computational domain i.e. all the boundaries except for the inner boundary along the symmetry cut. Below in Figure 8a it can be seen how the BL:s are placed along the inner wall and how the mesh is coarser along the symmetry cut. Figure 8 as a whole shows how the mesh is constructed, from the top and from the side.

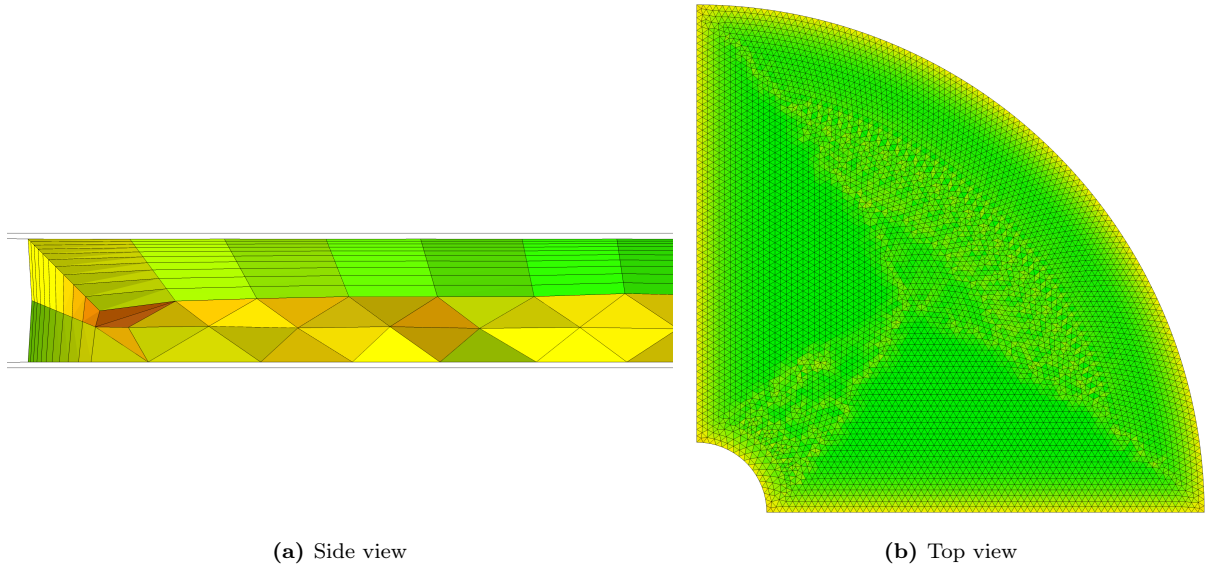


**Figure 8:** Shows the *Middle Mesh* from a side and a top view. In the side view the boundary layers can be seen.

## 3.2 Simulations

In total, 11 simulations had to be done to answer the questions asked within the aim of this project. The analysis will contain studying the rotor speed, the rotor radius and the thickness of the WGV. Beyond this, studies will also be done regarding the shape of the RS and regarding adding the HTC optimizers. To do these analyses, a reference model was defined from the earlier work of Eriksson et al. [13]. The relevant reference parameters can be found in Table 3, where reference values of rotor speed, rotor radius and thickness of WGV is specified in the first row, *Reference case*. In addition to this, the reference run will contain one slit as a quarter of a disc and no HTC optimizers will be applied, which is also marked in Table 3. For now, the quarter of a disc is the only design of GREC that has been investigated and used in prototypes. The alternative design, one eighth of a disc, will be explained further in Subsection 3.2.2. An explanation of the implementation of HTC optimizers follows in Subsection 3.2.3.

From the reference model, the quality of the mesh had to be validated, by the help of *Fine Mesh*, *Middle Mesh* and *Coarse Mesh*. By changing the mesh, from the finest to the coarsest, a choice was made by aggregating the quality of the mesh and the computational time. From these simulations, the *Middle Mesh* was selected and used for the following studies. A deeper explanation over the choice of mesh is presented in Subsection 3.2.1.

**Table 3:** An overview of the performed simulations. The first row presents the reference values that were used when nothing else is stated in the table. The rows below presents the changes that was made to the reference model for each different simulation.

Simulation name	Mesh name	Rotor speed [rpm]	Rotor radius [m]	Thickness of WGV [m]	Design of RS	HTC optimizer
Reference case		1500	0.29	0.008	1/4	Without
Fine Mesh	Fine					
Middle Mesh	Middle					
Coarse Mesh	Coarse					
Slow Rotor speed		500				
Fast Rotor speed		3000				
Short Rotor radius			0.145			
Long Rotor radius			0.58			
Thin WGV				0.005		
Thick WGV				0.011		
1/8 RS design					1/8	
HTC optimizer						With

Moving on to the parametric study, the part that is meant to be the foundation of the analysis within this project, a number of different parameters was changed in turns to see how this would influence the GREC. An overview of these changes of parameters can be seen in Table 3.

*Slow Rotor speed* and *Fast Rotor speed* both has the aim to determine guidelines for the rotor speed, by changing it to values both higher and lower than the reference value. All the values were chosen based on the background that the previous project, written by Eriksson et al. [13], used these rotor speeds. Compression between the two studies will thus be easier since they involve the same parameters.

Looking at the next simulations, the aim was to investigate how the size of engine, and especially the size of the WGV, affects the performance. *Short Rotor radius* and *Long Rotor radius* investigates the changes of rotor radius, while *Thin WGV* and *Thick WGV* investigates the change of thickness of WGV. Both reference dimensions were picked from the previous project by Eriksson et al. [13]. These are the same dimensions that is used in the Lab Model 2.0 of nilsinside AB. These dimensions were then changed to values both higher and lower. Relativity large changes were made to the dimensions to be able to see clear changes in the results and more easily highlight the trends. In addition, the dimensions of the rotor radius where picked in sync with the group working in parallel with the external heat transfer, to be able to share results between the two projects. Thus the factor of scaling is 2 when increasing the rotor radius and 0.5 when decreasing. While scaling the rotor radius, the rotor shaft radius is also scaled with the same factor.

After the parametric study the next step was to investigate two different designs of the RS, with matching designs of the fins. These two designs are described in Subsection 3.2.2. Lastly the potential of adding HTC optimizers was investigated. The concept and implementation of these HTC optimizerzers is described further under Subsection 3.2.3.

All the 11 presented simulations were compared and evaluated by the achieved pressure difference, the work that was possible to extract, a calculated efficiency and a HTC. The different simulations were chosen with the aim to simply for conclusions to be drawn, without having to run unnecessary simulations since every simulation requires relatively much computational power and time.

### 3.2.1 Verification and choice of mesh

When selecting the mesh used for the simulations, the quality of the mesh had to be correlated with the computational time. These parameters can be found in Table 4 and it can be seen that more elements implies longer computational time.

**Table 4:** For each reference condition from Table 3, the number of elements and the time it took to perform each simulation is displayed in this table. With more elements within the mesh comes a longer computational time.

Mesh name	Mesh No.	Elements [No.]	Time [s]	Time [h]
Fine	1	457 427	263 590	$\approx 73$
Middle	2	204 002	101 319	$\approx 28$
Coarse	3	73 686	26 453	$\approx 7$

Further, the quality of each mesh was calculated with the GCI-method presented in Section 2.4 and can be found in Table 5. Both the HTC and the pressure was qualitatively investigated.

**Table 5:** Calculated GCI parameters dependent in either the HTC or the pressure.

	HTC [W/m <sup>2</sup> K]	Pressure [kPa]
$\varphi_1$	87.33	4.51
$\varphi_2$	88.24	4.90
$\varphi_3$	71.83	5.13
GCI parameters		
GCI <sub>21</sub> [%]	0.14	7.1
GCI <sub>32</sub> [%]	1.6	2.8

The GCI values quantifies the error that arise due to discretisation in the domain and thereby low values is preferable. As can be seen in Table 5 the grid dependence overall is low since the calculated GCI values are low. Based on a consideration of both the GCI values and the time taken for the simulations a mesh could be chosen. For the HTC value the expected error when going from the middle mesh to the fine mesh is about 0.14 %, which is considered very low. For the pressure the error can be estimated to 7.1 % when comparing the middle and fine mesh. Therefore there is no point of choosing the fine mesh since the error is so low and the simulation time is about 2.5 times longer. Between the coarse and middle mesh the error can be estimated to about 1.6 % for the HTC value and 2.8 % for the pressure. Ultimately the middle mesh were chosen for its good compromise of accuracy and time.

### 3.2.2 Design of revolving shutter

The current prototype of the GREC, and the figures of the GREC that is presented so far in this report, all has one cold side and one warm side, with isolation in between. However, this way of designing the engine does not have to be the only way, and thereby one part of the project includes investigating an alternative design.

Both the original design and the alternative design is visualised in Figure 9, where 9a represents the original design, used in in the current prototype, and 9b represents an alternative design. The figures shows an schematic picture over both the conducting and isolating fins (to the right) and the RS with space for the WGV (on the left), for both alternatives.

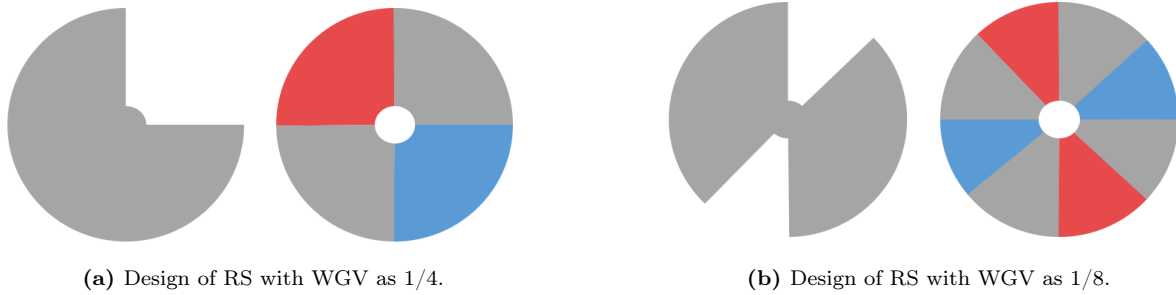


**Figure 9:** A schematic presentation showing the two different possible designs of the RS and associated fins. The red part represents the hot fins, the blue part represents the cold fins and the grey parts represents isolated components. For each design the RS is shown on the left and the conducting and isolating fins to the right.

The alternative design has two hot fins and two cold fins, with isolating fins in between each and every one of them, compared to only one hot fin and one cold fin for the original design. This results in the WGV containing a quarter of a disc in the original design, while it is halved in the alternative design and instead contains two eighths of a disc.

The purpose of the alternative design is to balance the weight of the RS more easily in the physical model and thereby avoid unnecessary friction when rotating. On the other hand, this change from a quarter to an eighth of a disc will probably also affect the model in other ways which will be investigated by changing the geometry of the WGV in the computational model.

### 3.2.3 Potential of optimizing the HTC

A turbulent flow has a higher Reynolds number which in theory will generate more heat transfer. It is thereby of interest to reach turbulent flow in the WGV to obtain a better performance of the GREC. A turbulent flow can be attained in multiple ways, where higher speed is one of them. Thus, a higher rotational speed could implement the performance in other ways as well, such as giving the WGV less time during heating, and the performance of the GREC can thereby be effected in other directions than intended by implementing a higher rotational speed.

An other alternative way to reach turbulent flow could be to install some kind of component in the WGV, which breaks the laminar flow into turbulent by disturbing the flow. This kind of component will from here on be referred to as a *HTC optimizer*. The design of such a HTC optimizer was not investigated in this project, but rather the potential of it. This was done by implementing a infinitely thin line of a solid material at the front of the WGV, see Figure 10. The idea is that this will disturb the flow and cause turbulence. In the simulation model, this thin line does not move along with the WGV and therefore more or less cuts through the WGV while it passes on the hot side. Due to limitations in how the HTC optimizer could be modeled, this phenomena could only be achieved on the hot side. This must be taken into consideration while studying the results. In reality on the other hand, a HTC optimizer will have to move along the movement of WGV to be possible to build mechanically. Thus, it will cut through the flow that enters the WGV from the dead volume, which is a flow that is not included in the computational model.



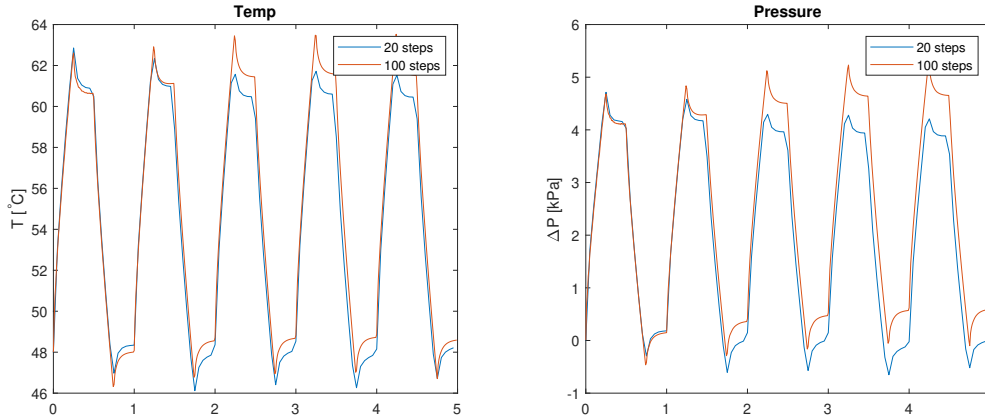


**Figure 11:** Shows how different time steps affect the solution. It can be seen that there is not much difference in mean temperature and pressure difference.

### 3.2.5 Validation run

To validate the performance of the model against the performance in reality, the results were compared to measured values of the first lab model. The setup for the lab model made use of a rotation speed of 90 RPM along with a hot storage side with  $40.5\text{ }^{\circ}\text{C}$  and a cold storage side with  $12.5\text{ }^{\circ}\text{C}$ . These temperature differences together with a WGV of 0.32 liter managed to produce approximately a pressure difference of 1 kPa [27, 28]. Further, an approximated value of the work generated from the lab model was also estimated to 0.6 W. Although these measures come from an early lab model, they could be used to indicate whether or not the results obtain within this project reflect the reality or not. Thus a *Validation run* will be performed with the same conditions as for the lab model.

In order to compare the work output between the lab model and the COMSOL model the COMSOL model geometry had to be slightly altered for the models to have the similar volume in WGV. The parameters that were changed were radius (from 29 to 25 cm), inner radius (4 to 5 cm), height (0.8 to 0.68 cm) and the number of layers were 1.

## 3.3 Post-processing

In this Section some method about how the post-processing is explained. All of the data processing have been carried out in MATLAB.

### 3.3.1 Pressure and temperature

Temperature and pressure is extracted from COMSOL as a domain average for every time step. Since each rotation consists of 20 steps, there is always 20 data points for each rotation. Over time, both temperature and pressure is cyclic and varies like a sine wave. To get the maximum potential temperature and pressure difference, a maximum and minimum for each rotation was extracted. In Figure 12 the temperature and pressure is plotted over time, normalized over the number of rotations. The minimum and maximum for each rotation is plotted as a blue and red star respectively.

fig

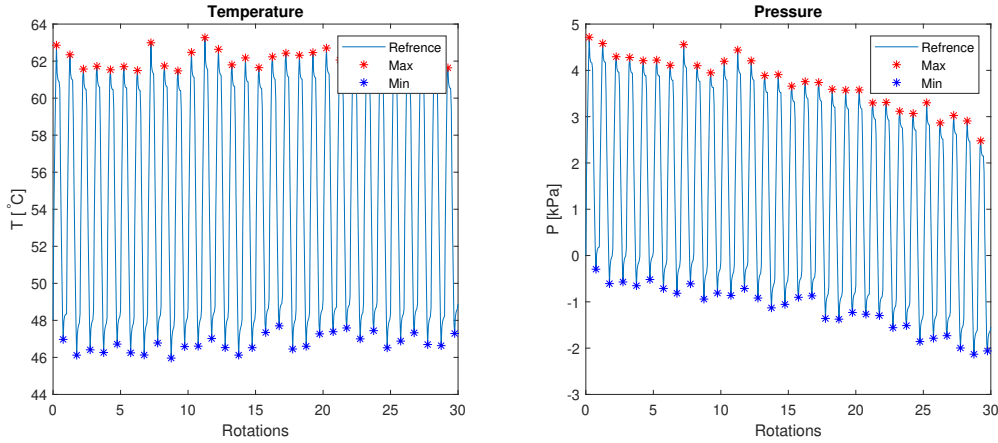


**Figure 12:** Shows temperature and pressure in the reference case as a function of time, normalised over the number of rotations. Red and blue stars highlights the maximum and minimum value of each rotation respectively.

The minimum value is then subtracted from the previous maximum value, to get the difference for each rotation. In Figure 13 the difference over time and mean difference is plotted. These mean values for temperature and pressure are later used to calculate the work done by the GREC. As can be seen in Figure 12 there is a downward trend for the pressure. However, while comparing the difference over time displayed in Figure 13, it can be seen that the downwards trend does not effect the mean value.

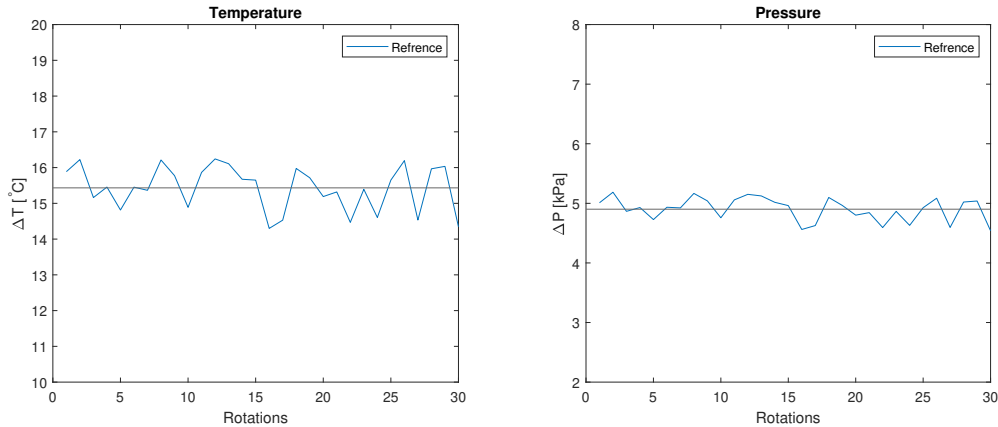


**Figure 13:** Shows the temperature and pressure straight differences of every rotation, of the reference case. The mean values of all rotation is marked by horizontal straight lines.

### 3.3.2 Heat transfer coefficient and rate of heat flow

The heat flux values are extracted for each time step from COMSOL, as a average value for the walls connected to the conductive fins. Calculations for the HTC value is done by Equation (16), displayed in Subsection 2.3.3, where  $T_{\infty}$  is estimated by taking the temperature at the center of the domain ( $T_c$ ). In theory the HTC value should go to infinity when the WGV is over the neutral fins, since the temperature difference should be as close to zero as possible. Therefore the extraction of HTC and rate of heat flow is done separately for the hot and cold side. Since every rotation is 20 steps and every quarter is five steps, the HTC and rate of heat flow of the hot side is extracted by taking the average for the fist five time steps in each rotation. The same is done for the cold side, but with time step 11 to 15.

### 3.3.3 Calculation of work

The available work was calculated using MATLAB following the Equations presented in chapter 2.2.1. Looking at Equation (4), the volume when the piston is pushed out ( $V_2$ ) and the volume when the piston is indented ( $V_1$ ) must be known.  $V_1$  was calculated geometrically following Equation (24) Below.

$$V_1 = \frac{\pi * (r^2 - r_i^2) * t * \text{layers}}{4} \quad (24)$$

The pressure  $p_1$  was calculated using the pressure fluctuations obtained from the performed simulations and is shown in Equation (25) below.

$$p_1 = p_{\text{atm}} + \frac{\Delta p}{2} \quad (25)$$

Using the assumption that the expansion of the piston is a isothermal process and the assumption that the pressure after the expansion ( $p_2$ ) is atmospheric the ideal gas law was used to calculate  $V_2$ , see Equation (26).

$$V_2 = V_1 * \frac{p_1}{p_2} \quad (26)$$

When the pressures and volumes had been calculated the values were put into Equation (5) and the boundary work for the volume expansion was obtained. Equation (6) was used to obtain the boundary work for the volume compression. However, in this case  $V_3 = V_2$  and  $V_4 = V_1$  from the previous calculation and the pressure used was assumed to be atmospheric pressure. By adding the boundary work from the two processes the work produced from one rotation of the rotating shutter was calculated. Multiplying the work per rotation with the number rotations per second and the number of layers gave the power output that the GREC can theoretically produce. In this study the number of layers were chosen to two, this was chosen since the current lab model has two layers.

If the useful power should be calculated the electrical power input to the external engine would have to be known. However, in this work the power input was not calculated and the useful power is thus not known.

# 4 Results

In this Chapter results from the simulation will be presented. In Figure 14 below the pressure difference from all cases is presented. Compared to the reference case the pressure difference for all variations follow the general trend that is expected, both based on the results from previous work and previous knowledge. Firstly, the slow rotor speed has higher pressure difference compared to the reference case and the fast rotor speed has the lowest pressure difference of the three. This was expected due to the time during heating, where the slower speed will have more time to heat up and thereby increase the pressure more. Secondly, the long rotor radius has higher pressure difference compared to the reference case and the short rotor radius, which was expected due to the bigger heating area in relation to the volume. Thirdly, the thin WGV has the highest pressure difference compared to the reference case and the thick WGV, which also was expected for the same reason with the bigger relative heating area. Further, the eighth of a disc has lower pressure difference which could be expected due to shorter time during heating. Lastly the HTC optimizer has higher pressure difference then the reference case which was the goal of adding them.

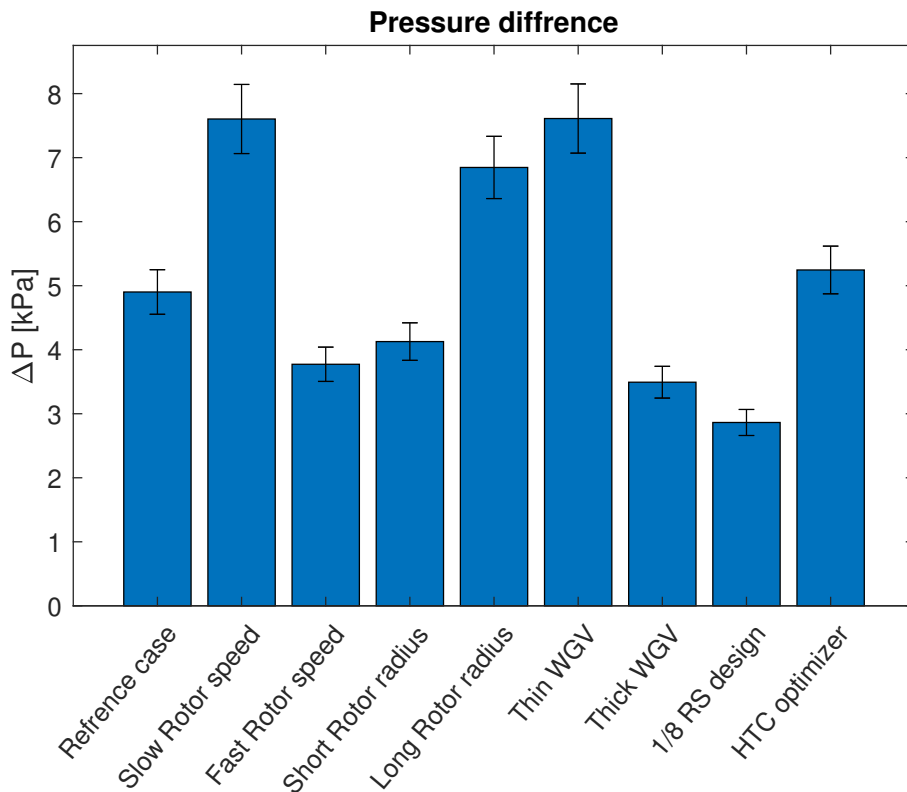


**Figure 14:** Pressure difference for the different simulations. The error bars show the grid induced error calculated with the GCI method. The pressure difference was taken for one rotation in all cases except for the 1/8 RS design where it was taken for half of one rotation.

From the pressure difference the work was calculated as presented in Subsection 2.2.1, and the result are presented in Figure 15. Among other things, it shows that the biggest amount of work is received with a long rotor radius and the least amount of work with the short rotor radius.

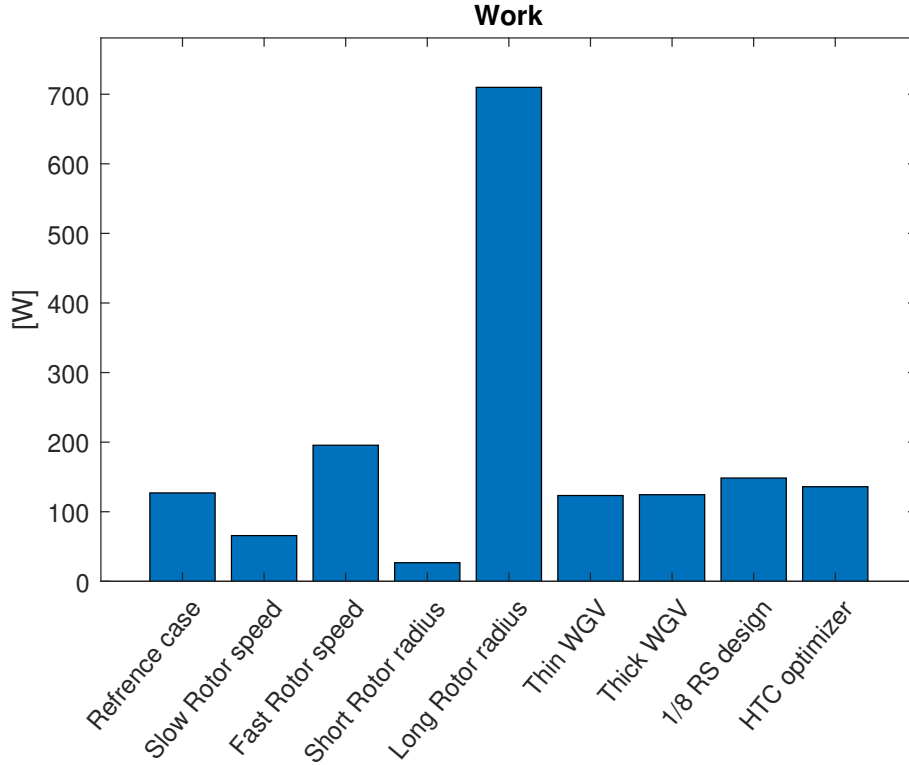


**Figure 15:** Calculated work from the pressure difference, for two layers in the GREC. The generated work depends on a number of parameters such as rate of heat flow and HTC.

The pressure difference and work output that are presented in the above diagrams are also presented with numbers in Table 6, together with the simulation time and the HTC for each simulation.

**Table 6:** Simulation time, pressure difference, HTC and work output from the reference case and the different simulations that were performed.

Simulation name	Description	Simulation time [h]	Pressure difference [kPa]	HTC [W/m <sup>2</sup> K]	Work [W]
Reference case		28	4.9	88.2	127.0
Slow Rotor speed	500 rpm	22	7.9	45.2	65.7
Fast Rotor speed	3000 rpm	29	3.8	122.7	195.6
Short Rotor radius	0.145 m	14	4.1	75.4	26.7
Long Rotor radius	0.58 m	50	6.8	114.4	709.9
Thin WGV	0.005 m	18	7.6	87.3	123.3
Thick WGV	0.011 m	21	3.5	59.8	124.5
1/8 RS design	1/8	19	2.9	119.4	148.4
HTC optimizer	With	27	5.2	96.0	136.0

The goal of the last simulation, the HTC optimizer, was to improve the turbulence in order to improve the HTC. Thus, it is interesting to study the turbulence over the domain for the simulation with a HTC optimizer and compare it with the reference case. The turbulence is visualised by the help of the EVR value in Figure 16. It can be seen that the simulation with the HTC optimizer has significantly higher EVR values in the front of the domain, seen from the direction of rotation, which indicates higher turbulence in this area.

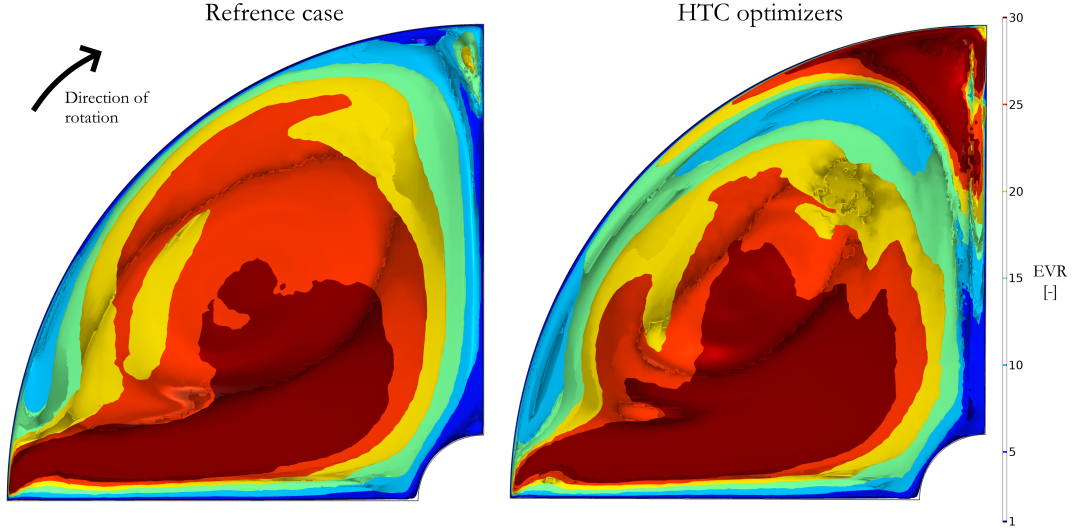


**Figure 16:** Shows isosurfaces of the EVR values over the domain, which indicates how turbulent the flow is. The HTC optimizer in the figure is located on the right side of the domain. The blue isosurface represent the lowest EVR and red represent the highest EVR.

## 4.1 Results for verification and validation

In this Section the results that are needed to perform verification and validation are displayed. Firstly the rate of heat flow is presented in Table 7. A positive rate of heat flow indicates that the energy is transferred into the GREC and the opposite is true when the rate of heat flow is negative [15].

**Table 7:** Rate of heat flow on the hot and the cold side, for one rotation. Rate of heat flow is positive when energy is transferred into the system and negative when energy is transferred out of the system.

	Rate of heat flow hot side [W]	Rate of heat flow cold side [W]
Reference case	454.4	-577.7
Slow Rotor speed	255.2	-335.7
Fast Rotor speed	687.7	-951.1
Short Rotor radius	89.0	-115.4
Long Rotor radius	2382.2	-3382.9
Thin WGV	442.5	-529.5
Thick WGV	419.8	-560.5
1/8 RS design	542.2	-697.2
HTC Optimizer	480.6	-607.6

Secondly the pressure difference and work output from the first lab model and the validation run is shown in Table 8. Values that belong to the lab model are extracted from an experiment meanwhile the values belonging to the validation run are obtained from the validation run simulation.

**Table 8:** Pressure difference and work output from the lab model and the validation run. The validation run uses the same conditions as for the lab model.

	Pressure difference [kPa]	Work [W]
Lab model	1	0.6
Validation run	6.8	3.25

# 5 Discussion

In this chapter the authors will discuss the work in regard to the method and results obtained, as well as discuss how well it relates to a physical model of the GREC. It will also be compared to the first physical lab model to try determining the validity of the COMSOL model and simulated results. Lastly, future works will be discussed and recommended from the authors point of view.

## 5.1 Method and model

The choice of using CFD for a project like this comes with some advantages. Firstly, it can be used to solve complex problems and thus not limits the user to simple problems where analytical solutions might not be possible. In the case of the simulations done in this project, a combination of thermodynamics and flow theory is needed to solve the problem and thus CFD is favorable. When the reference model is set, changes can most of the time be applied easily to investigate different geometrical and physical conditions. From the model it is also convenient to obtain parameters such as pressure, temperatures, rate of heat flow and HTC. However, using CFD also implies making some assumptions. Mass, momentum and energy must be conserved, since the calculations are based on Navier-stokes equations. These are assumptions built into the COMSOL program. Beyond this, more assumptions must be made while creating and running the model. From this, one can understand that although a good CFD model can bring good and accurate results seen from the computational point of view, it is not sure that these results correspond to reality.

One of these assumptions that could have an impact on the model is the choice of physics within COMSOL. Mainly it consider whether to assume that the fluid flow is laminar or turbulent. As described in Subsection 3.1.2, each different model has its own advantage and disadvantage and in this project the flow is assumed to be turbulent based on calculations of the Reynolds number. This forms the basis for the use of a turbulent model for the simulations. However, as mentioned in Subsection 2.3.1 and 2.3.2, it is hard to calculate and estimate the Reynolds number for the flow in the GREC. That is why it is interesting to investigate how the flow affects the results and if a turbulent flow is something that should try to be reached. This will further be discussed in Section 5.2.5.

Another assumption and simplification that had to be done in the model was the use of a time dependent temperature boundary condition for the insulating parts. In theory, no heat transfer is supposed to happen when the WGV is over the insulated fins. In reality however, there will be a temperature gradient from the hot and cold sides over the fins, this gradient was investigated in previous work [13]. This temperature gradient was impractical to model in this study, since the gradient is not known and is very dependent on different parameters such as thermal conductivity of the insulating fins. Thus the choice fell to mimic the theory as close as possible by choosing a fixed temperature as close as possible to the mean temperature of the WGV, when it enters the insulated area. Total heat transfer within the GREC can thus be influenced since heat transfer can occur in the insulating part if there is a temperature difference between the wall and the fluid. The set insulating temperatures was customized to fit the reference case and therefore the neutral zones were to be 5 °C higher/lower than the average temperature.

When other simulations were done, the temperature that entered the insulating part might have been higher or lower compared to the reference case and consequently the rate of heat flow over the hot and cold fins could be different. Since this approach was designed for the temperatures of the reference case, it did not match all other simulations perfectly. This was realised after a few simulations were completed and thus this has not been taken into account for all simulations and is therefore an area of improvement for future work. The simulations where this was adjusted for was the slow rotor speed and the validation run. The reason behind this was that the issue was discovered while conducting the validation run since a lot of heat transfer occurred at the insulating parts. In the case of the validation run, the temperature at the insulating parts had to be higher and lower respectively to imitate the behaviour of insulation. Improvements in the future could be done by trying to adjust the set temperature to each and every simulation.

By choosing to decompose the GREC all the way from the full engine to only investigating the WGV in the model, a lot of computational time could be saved. While limiting the model to only simulating the WGV saves computational time and complexity in the model, it also defines the boundary conditions that have to be used. These boundary conditions must be assumed to the best of our knowledge but does not fully represent the reality. This trade off of computational time and model complexity is something that permeate this work.

### 5.1.1 Mesh

When discussing computational time and complexity, it is unavoidable to bring up the meshing process. To continue were the last discussion ended, meshing quickly comes down to being a trade off between computational time and complexity. With a more complex mesh, a larger number of calculations will be done resulting in a more accurate model. The choice of using the middle mesh within this project is motivated in Subsection 3.2.1. Table 4 and Table 5 are used to evaluate the different meshes. Although the middle mesh is motivated for and used in this project, one could argue that the coarse mesh also performs in such a way that it could be considered a candidate for the mesh that should have been used. The GCI parameters are small when comparing the middle and the coarse mesh and the computational time is much less than the middle mesh. If time limit would have been a more important factor within this project, the coarse mesh could have been used with a little less accuracy but with a much shorter computational time. However, the actual HTC value differs with a little more than  $16 \text{ W/m}^2\text{K}$ . This in combination with the fact that the group could conduct simulation runs at nighttime finally set the choice on the middle mesh.

### 5.1.2 Verification

It is important to verify how well the model solves the problem that is to be solved. It was earlier calculated using the GCI-method that the mesh itself can lead to an error of roughly 7 % meaning that all of the results will have a degree of uncertainty to them. This error can be visualised in Figure 14. Furthermore, looking at how the model was built no work is actually extracted from the WGV, thus all that happens in the model when the RS rotates is that the air in the WGV heats and cools down in a cyclical manner, leading to a fluctuation in pressure. This means that the amount of heat put in to the system and leaving the system must be the same if the fundamental law of thermodynamics, stating that energy can not be created or destroyed, shall continue to apply. This given that the temperature in the WGV seems to have relatively

constant fluctuations and the average temperature also seems to be more or less constant, see Figure 12. However, looking at Table 7 it does not seem like the amount of heat flowing in to the WGV and flowing out are the same. It can be seen in all cases that the rate of heat flow on the cold side is greater than the warm side. This should not be the case since the RS is rotating at constant speed and therefore is in contact with the hot and cold side equal as long. The most likely reason to this unexpected behaviour is that the temperatures for the isolating segments in the time dependent temperature function are a bit off, meaning that heat is transferred to and from the WGV in these sections as well. The authors do not know how much this affects the model as a whole and if there are other problems contribute to this issue at the moment. What is clear however is that this issue effects the results which is something the reader must take into account.

It should also be stated that the temperature and pressure difference used in calculations is the average difference. Looking at Figure 13, it can be seen that the difference change slightly between every rotation. This should not be an issue for the results as the average is what matters over time. However, the rotations are steady so the difference between hot and cold side in the WGV should be constant. The reason why it changes probably has something to do with the mesh and the steps between each iteration in the simulation, i.e. the model does not solve everything perfectly and could use refinements.

### 5.1.3 Validation of model

Since there is only one early lab model built of the GREC, validation of the COMSOL model should be taken with a pinch of salt. It is assumed that the performance of the lab model is quite far from its real potential meanwhile the COMSOL model does assumptions that enhances its performance and thus performs better than the GREC would do in reality. The final GREC model should therefore show a performance that lays in between these two performances.

To perform the validation the values from the lab model have to be compared to the validation run, these values are displayed in Table 8. The setup with 40.5 °C on the hot side and 12.5 °C on the cold side, produced approximately a pressure difference of 1 kPa [27, 28] when implemented on the lab model. When these setup conditions where put in to the computational model, a pressure difference of 6.8 kPa was obtained. A value that is approximately seven time as high compared to the measured lab values is high, but the results shows that the values is in the same order of magnitude. This implies that the computational model is not to far from describing reality. One should also have in mind that the pressure difference received from this setup conditions, with relativity low temperatures, are in general very low and it is possible that the relative difference between the obtained pressure difference will decrease with higher temperature differences. Thus, it is not possible to investigate higher temperature differences since there are only results from one lab test available.

One reason to why there is such a big difference between the lab model and the simulation is that in the computational model the temperature is constant at the wall, which is not the case for the real model. In the lab model the temperature was measured at the hot and cold storage, i.e. the most extreme values. This means that towards the middle of the lab model there is a temperature gradient, which will in turn decrease the heat transfer to and from the WGV. To capture these temperature gradients and its interaction with the WGV a new model could be implemented where a whole layer, with both the fins and the WGV in the same model, could be investigated.

Further, the values of pressure difference fulfills the expectations that the computational model should give higher values than the lab model. This since the lab model has quite a lot of dead volume which will cancel out some of the pressure rise, since some of the dead volume is cooled while the WGV is heated up and vice versa. At the same time the computational model has no dead volume at all, which will give a higher pressure difference than what is actually possible to reach in reality. Based on this, the computational model should give a best case scenario and the lab model does describes a worst case scenario. The upcoming lab model and prototypes will probably end up somewhere in between these values, i.e. between 1 and 6.8 kPa for these setup conditions. The pressure difference from the computational model could theoretically generate a work of 3.25 W which also is significantly higher than the 0.6 W that the lab model was estimated to generate. Following the same reasoning as above this implies that a future lab model probably will generate somewhere between 0.6 W and 3.25 W.

### 5.1.4 Work output calculations

First of all the authors would like to say that it is very challenging to know which exact calculations applies when evaluating a new technology like this. The thought process behind the calculations of the work was mainly based on the Carnot heat cycle, see Figure 2, and statements on the web page of nilsinside AB. The Carnot cycle was used in the sense that the authors assumed that the air in the WGV first was heated, increasing the pressure. Then when the new pressure is reached and the piston is pushed out increasing the volume and decreasing the pressure until the pressure is the same as before. After this the process is the same but opposite when the air in the WGV is cooled. These assumptions brings a number of inaccuracies when comparing the model to reality. In reality the pressure and volume increase more or less simultaneously, and not in a step like fashion as assumed. Also, the assumption that there is atmospheric pressure at the start of the cycle and that the pressure fluctuates symmetrically around this atmospheric pressure does probably not represent reality without flaws. This said, it is hard to know how much these assumptions affect the results of the work output.

Looking at the work extraction through the piston this is also an area of great uncertainty. On nilsinside AB's web page it can be seen that one selling point of the GREC is that work can be extracted both as the piston is pushed out and pushed in [9]. Based on this the work generated in both directions was added together when calculating the work output in this project. Another reason that the works were added and not subtracted from each other was that there is an external motor driving the GREC, as external work is added to drive the heat engine. This in contrast to, for example, the Stirling engine where the works are subtracted from each other because a portion of the work must be used to push the piston back when no external motor is used. However, one could also argue that looking at it from a purely thermodynamic viewpoint of the Carnot cycle the amount of work is the area within the lines in Figure 2, meaning that with this viewpoint it should be subtraction between the works. Given the information the authors feel fairly confident in the decision to add the works together while still acknowledging the fact that it may be the wrong way to look at it.

From the results it can be seen in Table 6 that 127 W of work is generated in the reference case. Assuming that the external motor uses the same amount of power that was assumed in earlier work done by Eriksson et.al. [13], 24 W, it can easily be calculated that the amount of usable work is 103 W. This looks very promising for the technology especially looking at the work produced when the radius is increased. However, what one must keep in mind is that this model is highly idealised, not taking friction into account for example, meaning that a real model

would probably not come close to this level of performance. How much the assumptions affect the results and exactly how much power the external motor consumes is hard to determine which is one of many reasons why future work on a physical model must be conducted.

## 5.2 Parameter study

The main results from this project are compiled in Figure 14 and 15 along with Table 6. As a brief overlook, one can see that the pressure differences, HTC and work changes among other things. A slow rotor speed, long rotor radius and thin WGV all enhances the pressure difference. This however does not directly imply a higher work output. It can be seen that the simulation time differs quite a lot between different simulations. This occurs since different simulations lead to changes within the model and thus changes the amount of calculations that has to be done. For example a longer rotor radius and a thicker WGV leads to a larger model within COMSOL with more mesh elements and thus needs more calculations to solve.

### 5.2.1 Rotor speed

Starting to look at the presented result, the effect of the rotor speed is to be discussed. A slower rotor speed increases the pressure difference beyond the one of the reference case meanwhile a fast rotor speed lead to a lower pressure difference. This happens even though the HTC for the fast rotor speed is higher. The reason for this is that with a slower rotor speed, the WGV stays for a longer time over the hot and the cold side respectively. This results in a higher amount of heat transfer per rotation even though the HTC is lower. However, it is important to notice that since the fast rotor speed has a higher HTC, the heat transfer per unit of time is higher i.e. higher rate of heat flow.

Even though the pressure difference is increased for the slow rotor speed, it does not generate more work. In fact, a fast rotor speed with a lower pressure difference is what is preferred if more work is to be generated. The reason behind this is that a fast rotor comes with faster intervals of the pressure changes and thus resulting in a greater work output. This is also indicated by Table 7 that shows that the rate of heat flow is higher for the fast rotor speed. A higher work and rate of heat flow is true since these units are measured per second and not per rotation. This can be compared to the result of the pressure difference, displayed in Figure 14, that show the pressure difference per rotation and not per second. From this it is clear that rotation speed should be high if high work is desired. What is important to remember is that a higher rotation speed comes with its challenges. Aerodynamic losses such as drag and eventually shock waves could affect the efficiency of the GREC if rotation speeds are increased. It should also be of interest to investigate how a higher rotation speed would affect the demand of power delivered to the GREC from the external motor.

One question that could be asked is if it is reasonable for the RS to rotate at such a high RPM, especially when thinking about the project that will build a new lab model in the spring of 2023. 1500 RPM is fast, and considering that the first lab model move at around 90 RPM, this seems like a big leap to overcome. Both in terms of friction against the fins and in terms of aerodynamic losses. In future work a more reasonable rotational speed should be chosen and investigated.

## 5.2.2 Rotor radius

When studying the results from the change of rotor radius, it shows that a short short radius leads to both a lower pressure difference and a lower generated work. The main reason for this is that by increasing the rotor radius, several parameters change in favour for the performance of the GREC.

If the rotor radius is doubled it increases the area of the WGV with a factor of four. With such an increase it is understandable that more energy can be transferred from the hot and the cold side to and from the WGV. This can be seen in Table 7 since the rate of heat flow is high when the long rotor radius is used. In order to achieve the high work a lot of heat must be transferred to the WGV. A long rotor radius does not only increase the area but also the speed at the tip. Thus the new and increased volume will move with a higher speed due to the WGV:s rotational movement. With higher speed comes higher HTC and this also contributes to the increased heat transfer. These facts leads to a high work output. However, just like with an increased rotation speed the increase of rotor radius also has its practical challenges. Production of the GREC and mainly the RS will have to be done with high precision to avoid e.g., mechanical friction within the GREC. Further the balance of the RS would be a bigger challenge to solve. Since an increase of rotor radius also implies an increase of rotor speed at the tips, aerodynamic losses will have to be considered. Lastly, an increased of rotor radius will probably require more energy input from the electric motor due to the increased momentum.

## 5.2.3 Thickness of WGV

A thin WGV gives similar high pressure differences as with slow rotor speed, and in the same way a thick WGV gives similar low pressure differences as with fast rotor speed. The generated work however is more or less the same for the thin and the thick WGV. Although the thin WGV generates a higher pressure difference it is limited by the small volume when generating work. The opposite is true for the thick WGV where a larger volume is limited by the lower pressure differences that is generated. For a practical solution a thin WGV demands a precise production method of the RS. The RS could also be more fragile causing problem. Assuming that the dead volume is the same for both cases, this would be a greater percentile part with a thin WGV. A large proportion of dead volume decreases the efficiency of the GREC. This could be avoided with a thicker WGV. A thick WGV on the other hand could lead to the need of more work input to drive the WGV and also could lead to balance issues of the RS, on the other hand the RS will be stiffer with a thicker RS/WGV.

## 5.2.4 Changed design of revolving shutter

With the 1/8 RS design the pressure difference is decreased compared to the reference case. This is reasonable since the time that the WGV is adjacent to the hot and cold side is shorter. However, as can be seen in Figure 15, the generated work is improved. This can partly be explained by the fact that there are two cycles within one rotation of the RS and the total volume being the same in both cases. Since the pressure difference is slightly higher than half of the difference of the reference case, the two cycles in every rotation will generate more work than the reference case. Another reason for this could be that since the temperature change for the

1/8 RS design stays in a more narrow interval further from the temperatures of the surrounding hot and cold side. During one lap the total rate of heat flow is therefore higher and more work can be generated.

In practise the 1/8 RS design also has an advantage when looking at the balancing issue that the GREC has today. By having two separate WGV on the opposite sides of the RS, a balanced RS could be produced. Even though the generated work is higher compared to the reference case, one should remember that this work impacts the movement e.g., a piston. Instead of moving in and out during the time of one rotation, this piston would move in and out twice during the time of one rotation. The stroke length would also be shorter. In other words a 1/8 RS design would deliver work by moving a piston shorter but faster. Depending on the application of the GREC, this could be either advantageous or disadvantageous.

One disadvantage of the 1/8 RS design is the complexity of the construction of the GREC. Using this design would mean that two hot conducting fins must be placed opposite of each other and two cold conducting fins must also be placed opposite of each other in the other direction, see Figure 9b. This could potentially make the integration of the GREC into a system more challenging.

### 5.2.5 Use of HTC optimizers

Looking at Equation (14) it can be seen that a higher angular velocity and radius should increase the Reynolds number in the WGV leading to a higher HTC value and thus more heat transfer to the WGV. The higher heat transfer should lead to higher pressure fluctuations and thus higher work output. This seems to be the case looking at Table 6 where the average HTC value increases with higher rotor speed (angular velocity) and longer rotor radius. Thus, this increase of heat transfer could also be done by introducing the HTC optimizers. The HTC optimizers also shows a higher heat transfer and HTC, indicating on more turbulence. The same tendency also seems to be the case looking at the EVR values in Figure 16, which is a measurement of turbulence, where there is an increase of EVR in the part of the domain where the HTC optimizers are placed.

In regards to the method used to investigate the potential of HTC optimizers, there are a few things to point out. Firstly it should be mentioned that this part of the project was a bit challenging. Mainly due to the fact that the real physics within the GREC is not fully known. Not only are there no direct equations for calculating the Reynolds number for a flow like this, but also the amount of data from real world tests are limited. For this reason the Reynolds number had to be calculated with a big amount of uncertainty. From this result, a turbulent model was chosen and ended up being the point of reference. While investigating the potential of a turbulent flow, applying a direct laminar flow in the model instead of the chosen turbulent was tried but did not give the expected results. One reason for this is that COMSOL can give wrong answers if the flow in the model is turbulent and it is forced to do the calculations with the assumption that the flow is laminar. Thus another method had to be applied.

Instead of decreasing the turbulence the opposite approach was taken. By studying how an increase of turbulence would affect the model, the potential of an increased turbulent flow could still be indicated. The change from a turbulent flow to a more turbulent flow can be assumed to show lesser changes compared to the changes between a laminar and a turbulent flow. Thus it can be argued that if the flow in the GREC is laminar, the potential of increasing the flow to a turbulent flow would be higher than shown in this project.

## 5.3 Future work

In this Section the authors take a look at what work could be done to move the GREC project forward, and give recommendations on what they think are some of the most interesting aspects moving forward.

- *Look at implementation and design options for HTC optimizers:*

In this work the geometric implementation of HTC optimizers was not studied. However, by studying a case with a simple geometric distortion in the WGV, see Figure 10 and 16, it was shown that higher turbulence leads to higher HTC values and thus more work can potentially be generated.

There are many options to increase the turbulence in the boundary layer and thus increase the HTC. Geometric entities could be used in different configurations to break up the flow of the boundary layer. High pressure air could also be blown into the dead volume right before it enters the WGV and thus disturbing the flow entering the WGV. The authors of this report thus recommend future work on how the boundary layer can be broken up and thus increasing the HTC to the WGV.

- *How should the power be extracted?*

This work only explore the theoretical amount of generated work and does not go into how the work should be extracted from the WGV. A piston cylinder that is attached to the GREC is an option, but it may not be the optimal solution. Future work is needed to determine an efficient method of extracting the generated work. Looking into the possibility of using hydraulic options to extract the work would probably be of great value for the project. Using liquid filled pillows in the insulating fins to increase the area that the pressure acts on would increase the force the pressure difference can generate. A theoretically investigation of how the work could be extracted in the best way is a challenging task. A recommendation is therefore to try out different possible solutions on a lab model in the future.

- *Perform testing on a working physical model:*

The theoretical work output and thermal efficiencies are explored in this project. However, this is under optimal conditions where friction and other losses are neglected. This gives a good understanding of how different parameters affect the performance of the GREC qualitatively, for example that a larger radius gives a higher work output. On the other hand the validity of the exact values that are presented in the results is hard to determine. The results are especially tricky to determine because it is hard to know how well the physics in the COMSOL model reflect the real world physics. Therefore it would be valuable for the project with a working model to determine work output and efficiency quantitatively.

- *Can other fluids than air be used, and can condensation help to get more power?*

One question that is not explored at all in this report is how different fluids in the GREC would affect the results. In this work the authors just assume that the working fluid is air. However, using other fluids could increase or decrease the performance of the GREC. For example is the HTC dependent on the thermal conductivity of the fluid and thus a fluid with higher thermal conductivity should in theory increase the heat transfer to the the fluid and thus increase the work output. Therefore it would be interesting to look at how changing the working fluid would affect the results. It would also be interesting to look at fluids that partly change phase between the hot and cold side of the GREC and how this could affect the results.

- *How much power is needed to drive the rotating shutter?*

The external motor is outside the scope of this project. This said, it would be of great value for the broader GREC project to look into how the external motor needs to perform for the heat engine to a feasible option, and how it should be integrated into the GREC. This aspect is important to determine and investigate the efficiency of the GREC.

- *How does the dead volume affect the performance of GREC?*

The dead volume is in this project neglected to simplify the simulations and calculations. However it is something that could have impact on the performance in several ways. Firstly, it affects the total volume, which contains of both the WGV and the dead volume. Thus the dead volume will probably decrease the pressure difference due to it having a lower temperature when the WGV is heated and vice versa. Secondly, the dead volume is connected to the WGV by narrow slits where air will pass through. Thus the WGV is not actually a closed domain as simulated in this project, and there will in reality be both inflow and outflow from it. These flows could affect the turbulence in the WGV and thereby also the performance. Accordingly it would be interesting to investigate the dead volume further.

## 6 Conclusions

The performance of the GREC depend on a number of parameters discussed and studied within this project. The heat transfer within the GREC is complex and includes both thermodynamics and fluid dynamics. This makes it a challenging task to construct a model and perform simulations that reflect the real GREC.

In relation to the reference case, a slow rotor speed, a long rotor radius, a thin WGV or the use of HTC optimizers increase the pressure difference within the GREC. However, HTC is increased when a fast rotor speed, a long rotor radius, HTC optimizers or the 1/8 RS design is applied. These configurations with higher HTC also conduct in higher generated work. When higher work is generated, the rate of heat flow is also higher which implies that more heat and cooling must be available to reach this performance. Depending on the desired performance, e.g., amount of generated work or available heat, the design parameters can be chosen.

HTC optimizers can be applied to increase the HTC and with that the rate of heat flow, pressure difference and generated work. This increase in performance happens due to an increased turbulence within the WGV. Other measures to increase the HTC is to increase the rotation speed, increase the rotor radius and implementing a 1/8 RS design.

From the simulations performed within the scope of this project, the design proposal for the future is to build an engine that match the specific objective and preconditions for a special case. If delivering heat is no problem, then a large rotor radius is desirable to obtain a large amount of work. Future work is important to continue the studying of the GREC and evaluate its performance with other parameters such as number of layers that should be used.

# References

- [1] Cox L. East Antarctic glacier melting at 70.8bn tonnes a year due to warm sea water; 2022. Last accessed on 03-11-22. <https://www.theguardian.com/world/2022/oct/14/east-antarctic-glacier-melting-at-708bn-tonnes-a-year-due-to-warm-sea-water>.
- [2] Dominguez G. No longer the exception, extreme weather events becoming the norm; 2022. Last accessed on 03-11-22. <https://www.japantimes.co.jp/news/2022/08/29/asia-pacific/extreme-weather-new-normal/>.
- [3] BBC. Europe's drought the worst in 500 years - report; 2022. Last accessed on 03-11-22. <https://www.bbc.com/news/world-europe-62648912>.
- [4] Naturvårdsverket. Växthuseffekten förstärks; n.d. Last accessed on 23-06-22. <https://www.naturvardsverket.se/ammesomraden/klimatfakta/darfor-blir-det-varmare/vaxthuseffekten-forstarks/>.
- [5] Nations U. Paris Agreement; 2015. Last accessed on 23-09-22. <https://unfccc.int/process-and-meetings/the-paris-agreement/the-paris-agreement>.
- [6] Centre UCC. World is off track to meet Paris Agreement climate targets; 2021. Last accessed on 14-09-22. <https://unepccc.org/world-is-off-track-to-meet-paris-agreement-climate-targets/>.
- [7] Nilsinside. What is this Green Revolutionary news about?; n.d. Last accessed on 12-09-22. <https://nilsinside.com/nilsinside/Index-EN.html>.
- [8] Karlberg N. How the Green Revolution Energy Converter (GREC) works; 2021.
- [9] Nilsinside. The technology behind the GREC; n.d. Last accessed on 12-09-22. <https://nilsinside.com/nilsinside/Technology-EN.html>.
- [10] Nilsinside. Analysis of experiment; n.d. Last accessed on 13-09-22. [https://nilsinside.com/nilsinside/BREC\\_V2/LabAnalysis.html](https://nilsinside.com/nilsinside/BREC_V2/LabAnalysis.html).
- [11] Nilsinside. Status; n.d. Last accessed on 13-09-22. <https://nilsinside.com/nilsinside/status.html>.
- [12] Tzinis I. Technology Readiness Level; 2021. Last accessed on 13-09-22. [https://www.nasa.gov/directorates/heo/scan/engineering/technology/technology\\_readiness\\_level](https://www.nasa.gov/directorates/heo/scan/engineering/technology/technology_readiness_level).
- [13] Eriksson M, Magnusson O, Haglund L, Malmdal J, Edholm G. Theoretical Proof Of Concept For The GreenRevolution Energy Converter. The institution for economical and industrial development; 2022.
- [14] Hou X. The Carnot cycle; 2020. Last accessed on 20-08-15. [https://chem.libretexts.org/Bookshelves/Physical\\_and\\_Theoretical\\_Chemistry\\_Textbook\\_Maps/Supplemental\\_Modules\\_\(Physical\\_and\\_Theoretical\\_Chemistry\)/Thermodynamics/Thermodynamic\\_Cycles/Carnot\\_Cycle](https://chem.libretexts.org/Bookshelves/Physical_and_Theoretical_Chemistry_Textbook_Maps/Supplemental_Modules_(Physical_and_Theoretical_Chemistry)/Thermodynamics/Thermodynamic_Cycles/Carnot_Cycle).
- [15] Storck K, Karlsson M, Andersson I, Renner J, Loyd D. Formelsamling i termo- och fluidodynamik; 2012.

- [16] Hall N. Navier-Stokes equations; 2014. Last accessed on may 13 2021. <https://www.grc.nasa.gov/www/k-12/airplane/nseqs.html>.
- [17] COMSOL. Navier-Stokes equations; 2015. Last accessed on February 22, 2017. <https://www.grc.nasa.gov/www/k-12/airplane/nseqs.html>.
- [18] AB C. Turbulence Modeling; n.d. Last accessed on 12-10-22. [https://doc.comsol.com/5.5/doc/com.comsol.help.cfd/cfd\\_ug\\_fluidflow\\_single.06.085.html](https://doc.comsol.com/5.5/doc/com.comsol.help.cfd/cfd_ug_fluidflow_single.06.085.html).
- [19] Versteeg HK, Malalasekera W. An Introduction to Computational Fluid Dynamics; 2007.
- [20] Childs PRN. Chapter 5 - Rotor-Stator Disc Cavity Flow. In: Childs PRN, editor. Rotating Flow. Oxford: Butterworth-Heinemann; 2011. p. 127-76. Available from: <https://www.sciencedirect.com/science/article/pii/B9780123820983000056>.
- [21] Childs PRN. Chapter 4 - Introduction to Rotating Disc Systems. In: Childs PRN, editor. Rotating Flow. Oxford: Butterworth-Heinemann; 2011. p. 81-126. Available from: <https://www.sciencedirect.com/science/article/pii/B9780123820983000044>.
- [22] Çengel YA, Cimbala JM, Turner RH. Fundamentals of thermal-fluid sciences. McGraw Hill, LLC; 2012.
- [23] Neale A, Derome D, Blocken B, Carmeliet J. CFD calculation of convective heat transfer coefficients and validation - Part I: Laminar flow. 2006 01.
- [24] Celik IB, Ghia U, Roache PJ, Freitas CJ, Coleman H, Raad PE. Procedure for Estimation and Reporting of Uncertainty Due to Discretization in CFD Applications. Journal of Fluids Engineering. 2008 07;130(7). Available from: <https://doi.org/10.1115/1.2960953>.
- [25] Frei W. Which Turbulence Model Should I Choose for My CFD Application?; 2017. Last accessed on 12-10-22. <https://www.comsol.com/blogs/which-turbulence-model-should-choose-cfd-application/>.
- [26] The engineering toolbox. Altitude and speed of sound, temperature and pressure.; [https://www.engineeringtoolbox.com/elevation-speed-sound-air-d\\_1534.html](https://www.engineeringtoolbox.com/elevation-speed-sound-air-d_1534.html).
- [27] Karlberg N. Scaling, Size Matters; 2022.
- [28] Karlberg N. Analysis of Experiments; n.d. Last accessed on 02-12-22. [https://nilsinside.com/nilsinside/BREC\\_V2/LabAnalysis.html](https://nilsinside.com/nilsinside/BREC_V2/LabAnalysis.html).